TABLE II. Quantitative Evaluation of Neoplastic Lesions in Ventral Prostate of TRAP Rats Treated With ARBs

Treatment	No. of rats	LG-PIN	HG-PIN	AC
Experiment 1				
Control	11	7.2 ± 2.3	90.1 ± 2.2	2.7 ± 1.2
TS 2 mg/kg/day	12	11.9 ± 4.2*	86.7 ± 4.2	1.4 ± 0.4**
TS 10 mg/kg/day	12	12.5 ± 5.0**	85.9 ± 4.8*	1.6 ± 0.6**
Experiment 2				
Control	12	10.6 ± 4.5	83.1 ± 3.4	6.3 ± 2.8
CS 2 mg/kg/day	12	13.5 ± 5.9	82.6 ± 4.9	3.9 ± 2.1*
CS 10 mg/kg/day	12	18.4 ± 4.9**	78.9 ± 4.5	2.7 ± 1.2***
TS 10 mg/kg/day	12	22.5 ± 8.6***	75.0 ± 7.8**	2.5 ± 1.3***

Values (mean% ± SD) are the relative number of acini with histological characteristics against whole number of acini.
LG-PIN, low-grade prostatic intraepithelial neoplasia; HG, high grade; AC, adenocarcinoma; TS, telmisartan; CS, candesartan.
*P □ 0.05 versus control.
**P □ 0.01 versus control.
***P □ 0.001 versus control.

HG-PIN or adenocarcinoma were found in rats given telmisartan and high-dose candesartan (Tables I and II). The numbers of apoptotic cells in both the ventral and lateral prostate of rats treated with both telmisartan and candesartan were significantly increased as compared with the controls, whereas there was no obvious difference in Ki-67 labeling index (Fig. 1C,D). Immunoblot and immunohistochemical analyses clearly demonstrated activation of caspases 3 and 7 and a tendency for inactivation of p38 MAPK in the ventral prostate of rats treated with both candesartan and telmisartan, as likewise shown in experiment 1 (Fig. 1F,H,J). There was no significant difference in AT1R expression among the groups (Fig. 1L).

Suppressive Effects of ARBs on the Expression and Transcriptional Activity of Androgen Receptor (AR)

We examined the effects of ARBs on AR expression because previous clinical studies demonstrated that ARBs have potential to decrease serum PSA level in prostate cancer patients. AR protein expression was down-regulated in the ventral prostate of TRAP rats while SV40 T antigen protein and AR mRNA expression did not differ among the groups (Fig. 2A,B). Immunohistochemical analysis revealed that all prostate epithelial cells, including neoplastic and normal-looking cells, expressed SV40 T antigen at almost similar levels (Fig. S4A). Real-time RT-PCR of the androgen responsive gene, GK11, known as an ortholog of human PSA, demonstrated significant down-regulation by ARB treatment while probasin expression levels showed no clear alteration (Fig. S4B,C). In human prostate cancer and prostate epithelial cells, all cells used in the present study expressed both AT1R and AT2R but its levels were variable (Table S5). In LNCaP cells, ARBs repressed both AR and PSA protein expression although real-time RT-PCR analysis of the AR gene showed no obvious difference among treatments (Fig. 2C,E). ARBs also suppressed both AR and PSA expression in VCaP cells, androgen-independent prostate cancer cells harboring wild type AR (Fig. 2D). The suppressive effect of ARBs on AR protein expression was blocked by the proteasome inhibitor, MG132, suggesting that a proteasome-dependent pathway is involved in ARB-induced AR protein down-regulation (Fig. 2F). Subsequent luciferase reporter assays clearly demonstrated significant inhibition of AR transcriptional activity, this finding being considered to simply reflect down-regulation of AR protein expression by ARBs (Fig. 2G).

In RWPE-1 cells, normal epithelial cells from the peripheral zone of the human prostate immortalized with human papilloma virus 18, candesartan did not affect cell growth while high-dose of telmisartan attenuated cell proliferation (Fig. S5).

Estrogen Receptor □ (ER□) Upregulation by ARBs in Prostate of TRAP Rats and Human Prostate Cancer Cell Lines

To further investigate the downstream molecule(s) of AT1R responsible for suppression of prostate carcinogenesis, we performed microarray analysis using ventral prostate tissue of TRAP rats. According to comprehensive mRNA profiling by DNA microarray, 28 genes were up-regulated and 43 were down-regulated in the telmisartan treatment group over the control (Delta = 0.340; Fig. S6). Table S6 showed significant genes detected microarray analysis. Among these genes, we focused on ERβ as one of the genes up-regulated by ARB treatment because the majority

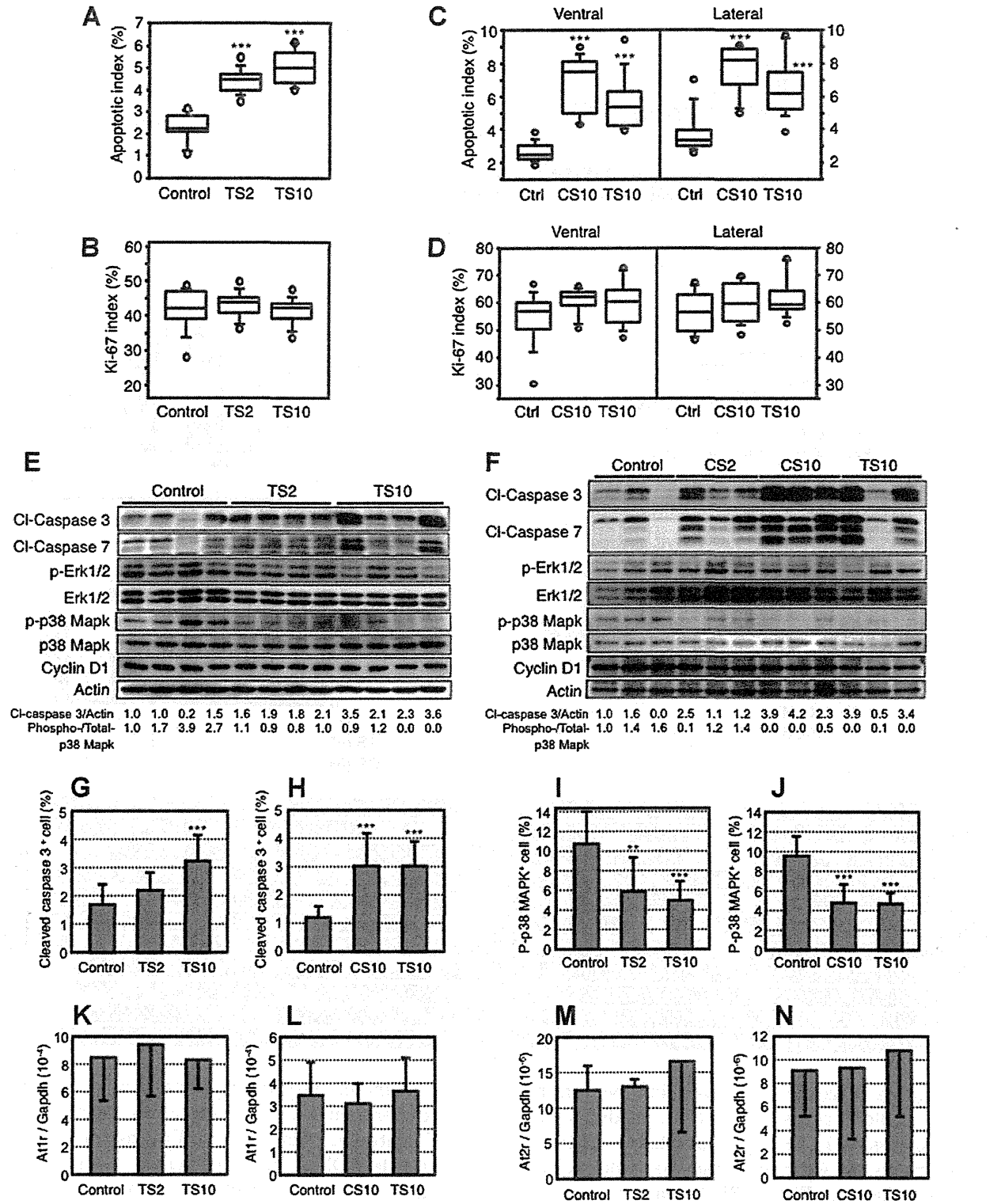
A
Apoptotic index (%)
Control TS2 TS10
C
Ventral
Lateral
Apoptotic index (%)
Ctrl CS10 TS10
Ctrl CS10 TS10
B
Ki-67 index (%)
Control TS2 TS10
D
Ventral
Lateral
Ki-67 index (%)
Ctrl CS10 TS10
Ctrl CS10 TS10
E
Control TS2 TS10
Cl-Caspase 3
Cl-Caspase 7
p-Erk1/2
Erk1/2
p-p38 Mapk
p38 Mapk
Cyclin D1
Actin
Cl-caspase 3/Actin 1.0 1.0 0.2 1.5 1.6 1.9 1.8 2.1 3.5 2.1 2.3 3.6
Phospho-/Total-p38 Mapk 1.0 1.7 3.9 2.7 1.1 0.9 0.8 1.0 0.9 1.2 0.0 0.0
F
Control CS2 CS10 TS10
Cl-Caspase 3
Cl-Caspase 7
p-Erk1/2
Erk1/2
p-p38 Mapk
p38 Mapk
Cyclin D1
Actin
Cl-caspase 3/Actin 1.0 1.6 0.0 2.5 1.1 1.2 3.9 4.2 2.3 3.9 0.5 3.4
Phospho-/Total-p38 Mapk 1.0 1.4 1.6 0.1 1.2 1.4 0.0 0.0 0.5 0.0 0.1 0.0
G
Cleaved caspase 3 + cell (%)
Control TS2 TS10
H
Cleaved caspase 3 + cell (%)
Control CS10 TS10
I
P-p38 MAPK+ cell (%)
Control TS2 TS10
J
P-p38 MAPK+ cell (%)
Control CS10 TS10
K
At1r / Gapdh (10-4)
Control TS2 TS10
L
At1r / Gapdh (10-4)
Control CS10 TS10
M
At2r / Gapdh (10-6)
Control TS2 TS10
N
At2r / Gapdh (10-6)
Control CS10 TS10

Fig. 1.

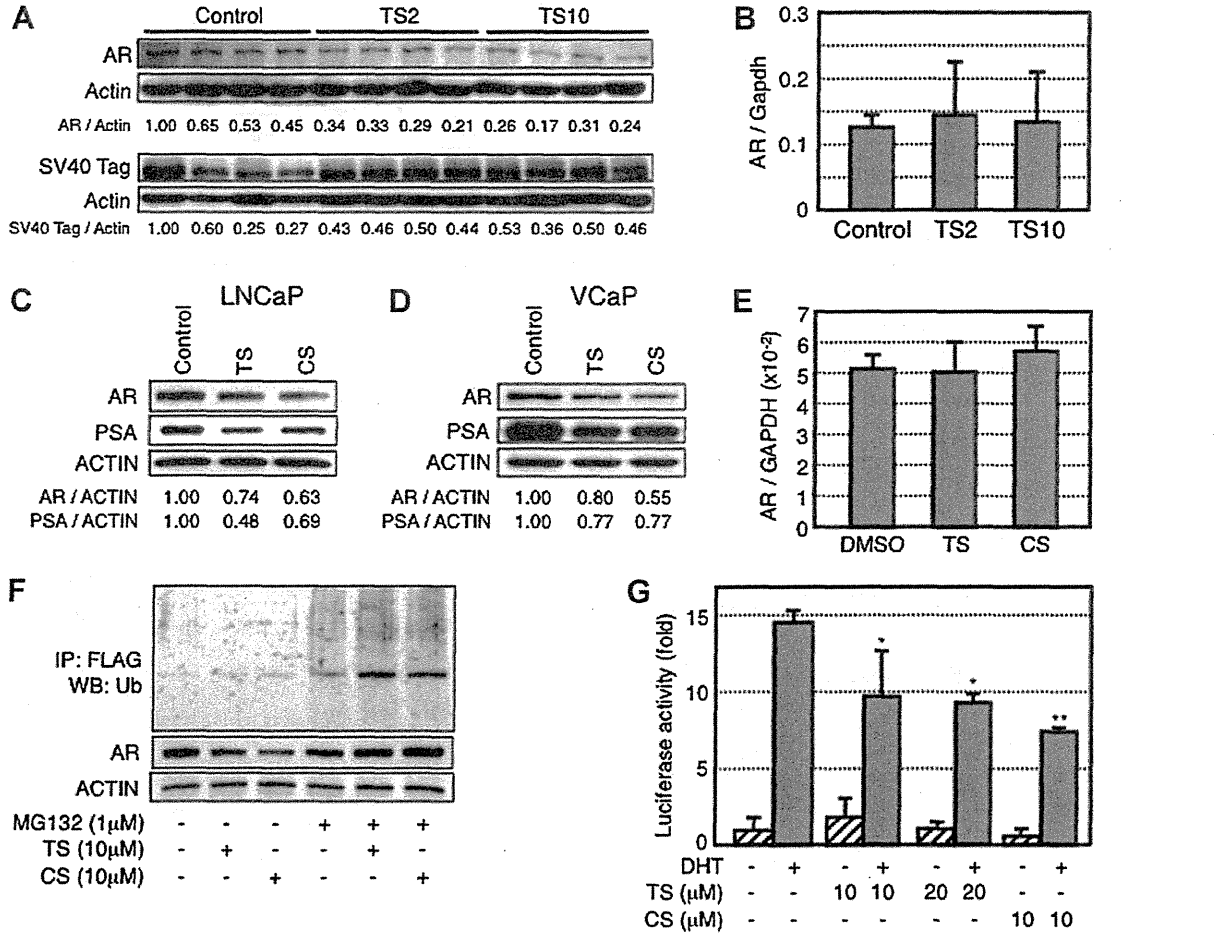

Fig. 2.

of the genes other than ERβ were involved in the regulation of blood pressure. First, we needed to confirm ERβ expression in TRAP rat prostate in both in vivo experiments, as we have done. As expected, significant elevation of ERβ mRNA was observed in the ventral prostate of TRAP rats by quantitative RT-PCR (Fig. 3A,B), and a similar phenomenon was found in LNCaP cells exposed to ARBs (Fig. 3C).

Up-Regulation of ER Induce Suppression of AR Transcriptional Activity and Prostate Cancer Cell Growth

Luciferase reporter assay demonstrated that forced expression of ERβ in LNCaP cells clearly inhibited AR-mediated transcriptional activity in both ligand-dependent and -independent manners (Fig. 3D). Treatment with selective ERβ agonists, diarylpropionitrile (DPN) and biochanin A, suppressed both growth and AR-mediated transcriptional activity of LNCaP cells as did ARBs (Fig. 3E,F). Immunoblot analysis revealed that selective ERβ agonists down-regulated PSA expression but AR expression was increased in LNCaP cells (Fig. 3G). Selective ERβ agonist-induced cell growth suppression was blocked by siRNA-mediated knock-down of AR expression, suggesting that the suppressive action of ERβ was via the AR signaling pathway (Fig. 3H). Knock-down of ERβ expression by siRNA did not affect on cell

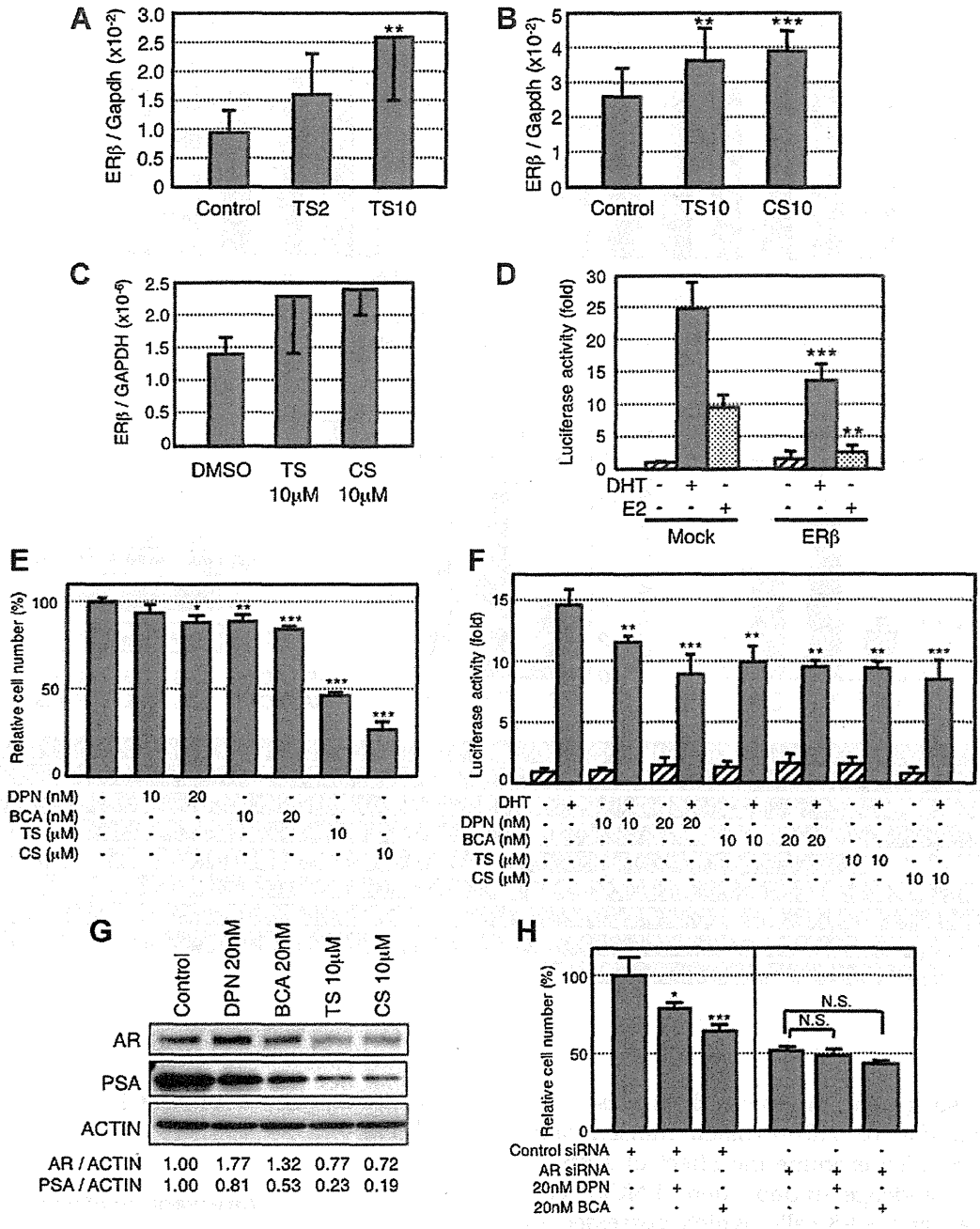

Fig. 3. β A B C β D β β E β E β β G β H β *P

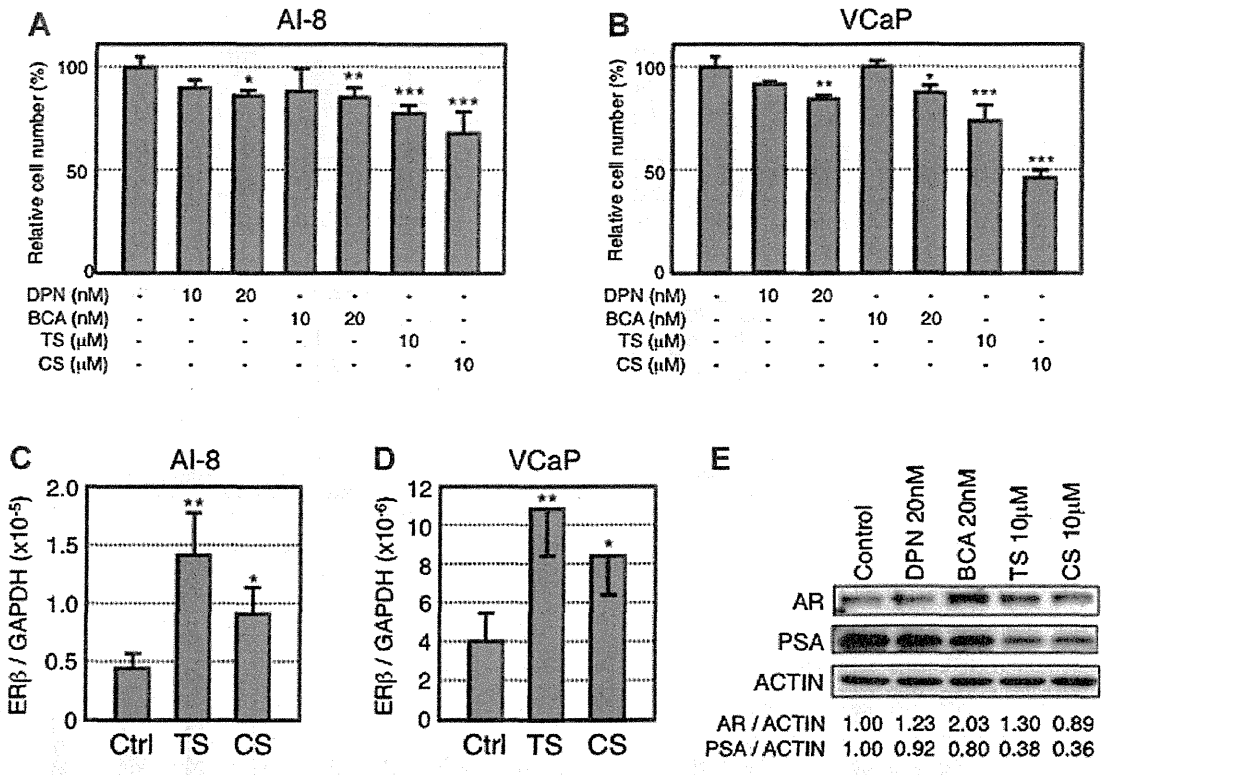

Fig. 4.

proliferation, suggesting the role of ERβ was a mild additional modifier on AR-mediated transcriptional activity (Fig. S7). To examine the effect of ARBs on the growth of androgen-independent LNCaP cells, we used VCaP and AI-8 cells, which possessed the highest PSA expression among the four sublines (Fig. S1C). Selective ERβ agonists as well as ARBs inhibited cell proliferation of both AI-8 and VCaP cells (Fig. 4A,B). Immunoblot analysis revealed that AR expression was increased while PSA was decreased by treatment with selective ERβ agonists in AI-8 cells (Fig. 4E). On the other hand, ARBs clearly repressed PSA expression although the AR protein level was slight increased with telmisartan (TS) and decreased with candesartan (CS) treatment compared with the no-treatment control. These results are in marked contrast to the findings seen in androgen-dependent parental LNCaP cells as shown in Fig. 3G. Up-regulation of ERβ mRNA expression by ARB treatment was observed in both AI-8 and VCaP cell (Fig. 4C,D).

Intervention Study

Background data of the patients are shown in Table S7. aPSA-DT was significantly longer than ePSA-DT in both the olmesartan-treated patients (see Materials and Methods Section), median 436.3 versus 128.7 days ($P = 0.004$; Fig. 5A). However, the ratio of aPSA-DT/ePSA-DT was significantly longer in olmesartan-treated patients (3.36 times) than in control patients (1.80 times) ($P = 0.0156$), indicating that olmesartan treatment could delay PSA progression (Fig. 5B). Fig. 5C shows that $TTPP_{1.0}$ from biochemical failure (0.2 ng/ml) to over 1.0 ng/ml in olmesartan-treated patients was significantly longer than that in control patients (no treatment; $P = 0.026$). Similarly, the time for PSA progression from the PSA nadir to over

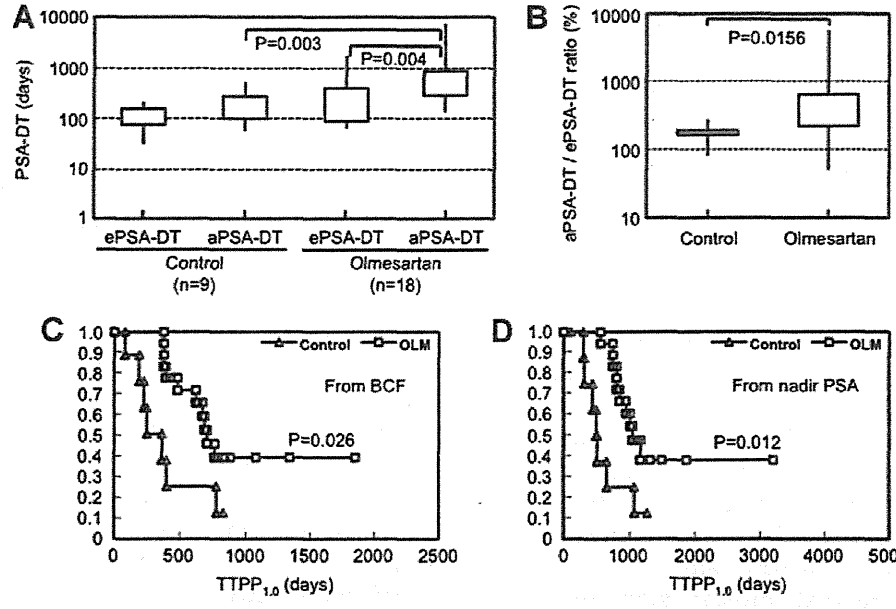

Fig. 5.

1.0 ng/ml in olmesartan-treated patients was significantly longer than that in control patients ($P = 0.012$) as shown in Fig. 5D.

DISCUSSION

It is widely accepted that there are multiple processes in the development of cancer; that is, initiation, promotion and progression. In 1976, Sporn proposed "cancer chemoprevention" as a strategy for prevention of cancer to delay the development of clinically evident disease by suppression of progression from precancerous lesions to invasive cancer by giving natural or synthetic compounds [17]. Prostate cancer is known to be strongly associated with aging, that is, about three-quarters of cases worldwide occur in men aged 65 years or more [18]. Therefore, prostate cancer is an attractive target for cancer chemoprevention because of the high population incidence and long latent period, and several dietary factors as well as genetic background have been linked to risk and progression of prostate cancer [19,20]. In fact, a large number of observational or intervention studies have been conducted using vitamins, phytochemicals, and minerals [21,22]. Moreover, three large scale randomized clinical trials, SELECT (Selenium and Vitamin E Cancer Prevention Trial) [23], PCPT (Prostate Cancer Prevention Trial) [24], and REDUCE (Reduction by Dutasteride of Prostate Cancer Events) [25], have been completed, and the latter two trials using 5α-reductase inhibitors showed a reduction of prostate cancer risk, although adverse effects including sexual dysfunction were observed. From the viewpoint of sexual dysfunction, ARB could restore rather than induce these side effects [26–28].

The present study demonstrated suppressive effects of ARBs on prostate tumor progression in an in vivo animal model, with decrease in the development of both HG-PINs and adenocarcinoma and consequent increase in LG-PINs in the ventral prostate. We have validated the chemopreventive effects of various chemicals including anti-androgens using our TRAP rats [14,15,29,30]. This transgenic rat is characterized by the sequential development of prostatic lesions, that is, LG-PINs, HG-PINs and adenocarcinomas in almost all acini in the entire ventral and lateral lobes. The SV40 T antigen used in the transgene of the TRAP rat acts as a potent oncoprotein to strongly stimulate cell growth and the development of adenocarcinomas in almost all acini in the entire prostatic lobes through inhibiting both the pRB and p53 tumor suppressor pathways. Since expression of SV40 T antigen is regulated by the androgen-dependent probasin promoter, it is speculated that cancer

development in TRAP rats is very sensitive to chemicals that modulate the AR axis, including the endogenous androgen level. The possibility that suppressive effects of ARBs were due to down-regulation of the transgene expression could be excluded by the data on SV40 T antigen expression shown in Figures 2A and S4A. The in vivo finding that ARBs not only down-regulated AR protein but also suppressed the androgen responsive gene, GK11, an ortholog of human PSA, at the mRNA level, provided evidence that ARBs functionally suppressed the AR pathway in prostatic lesions of TRAP rats. Thus, the present study highlighted that the main pathway responsible for attenuation of prostate carcinogenesis by ARBs is the AR signal pathway through suppression of AR-mediated transcriptional activity by both AR down-regulation and ERβ up-regulation, as well as inactivation of the p38 MAPK pathway.

ERβ is known to regulate prostate gland growth as an antiproliferative receptor [31]. This study demonstrated that ERβ is one of the downstream molecules of AT1R, and the ERβ signal transduction pathway plays an important role in the mechanisms of suppression of prostate carcinogenesis by ARBs. Genistein and deizein, major components of soybean isoflavone, have been shown to exert suppressive effects on rat prostate carcinogenesis [32], and these compounds are known to bind ERβ and to have ERβ agonistic activity [33]. Gamma-tocopherol has also demonstrated an inhibitory effect on prostate carcinogenesis in TRAP rats by activation of caspase signaling [15] and it is speculated that the ERβ signal pathway might be involved in these inhibitory effects because gamma-tocotrienol was recently revealed to induce apoptosis by activation of caspase 3 and ERβ signaling [34]. The latest report suggests that ERβ exerts a pivotal role in sustaining the epithelial phenotype and suppressing the acquisition of epithelial-mesenchymal transition and aggressive characteristics of prostate cancer [35]. This accumulating evidence suggests that modulators of ERβ might be potential chemopreventive or chemotherapeutic agents.

Among the ARBs used here, telmisartan demonstrated PPARγ activation while candesartan and olmesartan did not [36]. Additionally, olmesartan is known to increase angiotensin 1–7 levels through activation of angiotensin converting enzyme 2 [37]. No toxic effects were observed in TRAP rats treated with candesartan while significant suppression of body weight gain was found with the high-dose telmisartan. These phenomena are presumably PPARγ-related and similar effects of telmisartan have been reported previously [38,39]. However, it has been proven to also potentiate the signaling of PPARα or PPARδ in mice [40,41], and PPARδ activation is deeply involved in the prevention of body weight gain by telmisartan [42].

Androgen deprivation therapy remains the gold standard first-line treatment for prostate cancer; however, most tumors gradually acquire a castration-resistant phenotype. Several signal pathways responsible for the pathogenesis of CRPC have been elucidated, and growth and survival of CRPC continue to depend on a functional AR signal pathway that is adapted to a microenvironment of low androgen levels [43,44]. At present, several agents targeting AR signaling have been developed, such as a new type of anti-androgens, CYP17 inhibitors, HSP90 inhibitors, histone deacetylase inhibitors, and tyrosine kinase inhibitors [45]. The present data suggest that ARBs are also candidates for suppressor drugs of the AR signal pathway by attenuating AR-mediated transcriptional activity.

Our previous report indicated that ARBs have the potential to decrease or stabilize PSA level of patients with CRPC and inhibit the occurrence of symptoms such as bone pain [9]. These effects seemed to be due to the anti-inflammatory and anti-angiogenesis activity of ARB. In this study, we examined whether ARBs could clinically affect the growth of hormone-naïve cancer cells. In general, it has been reported that aPSA-DT was longer than ePSA-DT from the nadir of biochemical failure (BCF), PSA 0.2 ng/ml [46]. However, olmesartan treatment markedly prolonged PSA-DT in patients with BCF, that is, PSA □ 0.2 ng/ml after RP, in comparison with non-treated patients (control patients). It is well known that PSA-DT after RP is strongly associated with the risk of cause-specific mortality [47], and is a predictor of development of metastasis [48–50]. In the present study, administration of olmesartan prolonged aPSA-DT 2 fold compared with non-treated patients. These clinical data are consistent with in vivo and in vitro data showing that ARBs have the property to suppress the progression of prostate cancer associated with PSA decrease.

Interspecies scaling is commonly used to extrapolate doses from animal experiments to humans. It is known that plasma concentrations are better than dose levels for the interpretation of animal studies. An approximately five times higher dose in rats compared with human dose level is necessary to reach similar average steady-state plasma levels [51]. Moreover, the 0.75 power of body weight method is conventionally used in scaling [52,53]. The formula is (mg dose in rat)/(rat body weight)$^{3/4}$ = (mg dose in human)/(human body weight)$^{3/4}$, and this can be rewritten as (mg/kg/day dose in rat) × (rat body weight)$^{1/4}$ = (mg/kg/day dose in human) × (human body weight)$^{1/4}$. Applying this formula in the present

26. Dusing R. Effect of the angiotensin II antagonist valsartan on sexual function in hypretensive men. Blood Press Suppl 2003; 2:29–34.
27. Nomura M, Nishii H, Ozaki Y, Fujimoto N, Matsumoto T. An angiotensin II receptor blocker increases sexual behavior in type 2 diabetic mice. Physiol Behav 2007;91:223–228.
28. Yang R, Yang B, EWen Y, Fang F, Cui S, Lin G, Sun Z, Wang R, Dai Y. Losartan, an angiotensin type I receptor, restores erectile function by downregulation of cavernous renin-angiotensin system in streptozocin-induced diabetic rats. J Sex Med 2009; 6:696–707.
29. Cho YM, Takahashi S, Asamoto M, Suzuki S, Tang M, Shirai T. Suppressive effects of antiandrogens, finasteride and flutamide on development of prostatic lesions in a transgenic rat model. Prostate Cancer Prostatic Dis 2007;10:378–383.
30. Tang M, Ogawa K, Asamoto M, Hokaiwado N, Seeni A, Suzuki S, Takahashi S, Tanaka T, Ichikawa K, Shirai T. Protective effects of citrus nobiletin and auraptene in transgenic rats developing adenocarcinoma of the prostate (TRAP) and human prostate carcinoma cells. Cancer Sci 2007;98:471–477.
31. Weihua Z, Mäkelä S, Andersson LC, Salmi S, Saji S, Webster JI, Jensen EV, Nilsson S, Warner M. Gustafsson J-Å. A role for estrogen receptor β in the regulation of growth of the ventral prostate. Proc Natl Acad Sci USA 2001;98:6330–6335.
32. Kato K, Takahashi S, Cui L, Toda T, Suzuki S, Futakuchi M, Sugiura S, Shirai T. Suppressive effects of dietary genistin and daidzin on rat prostate carcinogenesis. Jpn J Cancer Res 2000;91:786–791.
33. Escande A, Pillon A, Servant N, Cravedi J-P, Larrea F, Muhn P, Nicolas J-C, Cavailles V, Balaguer P. Evaluation of ligand selectivity using reporter cell lines stably expressing estrogen receptor alpha or beta. Biochem Pharmacol 2006;71:1459–1469.
34. Comitato R, Nesaretnam K, Leoni G, Ambra R, Canali R, Bolli A, Marino M, Virgili F. A novel mechanism of natural vitamin E tocotrienol activity: Involvement of ERβ signal transduction. Am J Physiol Endocrinol Metab 2009;297:E427–E437.
35. Mak P, Leav I, Pursell B, Bae D, Yang X, Taglienti CA, Gouvin LM, Sharma VM, Mercurio AM. ERbeta impedes prostate cancer EMT by destabilizing HIF-1alpha and inhibiting VEGF-mediated snail nuclear localization: Inplications for Gleason grading. Cancer Cell 2010;17:319–332.
36. Kurtz TW, Pravenec M. Antidiabetic mechanisms of angiotensin-converting enzyme inhibitors and angiotensin II receptor antagonists: Beyond the renin-angiotensin system. J Hypertens 2004;22:2253–2261.
37. Agata J, Ura N, Yoshida H, Shinshi Y, Sasaki H, Hyakkoku M, Taniguchi S, Shimamoto K. Olmesartan is an angiotensin II receptor blocker with an inhibitory effect on angiotensin-converting enzyme. Hypertens Res 2006;29:865–874.
38. Sugimoto K, Qi NR, Kazdova L, Pravenec M, Ogihara T, Kurtz TW. Telmisartan but not valsartan increases caloric expenditure and protects against weight gain and hepatic steatosis. Hypertension 2006;47:1003–1009.
39. Araki K, Masaki T, Katsuragi I, Tanaka K, Kakuma T, Yoshimatsu H. Telmisartan prevents obesity and increases the expression of uncoupling protein 1 in diet-induced obese mice. Hypertension 2006;48:51–57.
40. Clemenz M, Frost N, Schupp M, Caron S, Foryst-Ludwig A, Bohm C, Hartge M, Gust R, Staels B, Unger T, Kintscher U. Liver-specific peroxisome proliferator-activated receptor alpha target gene regulation by the angiotensin type 1 receptor blocker telmisartan. Diabetes 2008;57:1405–1413.
41. He H, Yang D, Ma L, Luo Z, Ma S, Feng X, Cao T, Yan Z, Liu D, Tepel M, Zhu Z. Telmisartan prevents weight gain and obesity through activation of peroxisome proliferator-activated receptor-delta-dependent pathways. Hypertension 2010;55: 869–879.
42. Fleshner N, Fair WR, Huryk R, Heston WDW. Vitamin E inhibit the high-fat diet promoted growth of established human prostate LNCaP tumors in nude mice. J Urol 1999;161:1651–1654.
43. Attar RM, Takimoto CH, Gottardis MM. Castration-resistant prostate cancer: Locking up the molecular escape routes. Clin Cancer Res 2009;15(10):3251–3255.
44. Bonkhoff H, Berges R. From pathogenesis to prevention of castration resistant prostate cancer. Prostate 2010;70:100–112.
45. Chen Y, Sawyers CL, Scher HI. Targeting the androgen receptor pathway in prostate cancer. Curr Opin Pharmacol 2008;8: 440–448.
46. Teeter AE, Presti JCJ, Aronson WJ, Terris MK, Kane CJ, Amling CL, Freedland SJ. Does early prostate-specific antigen doubling time (ePSADT) after radical prostatectomy, calculated using PSA values from the first detectable until the first recurrence value, correlate with standard PSADT? A report from the Shared Equal Access Regional Cancer Hospital Database Group. BJU Int 2009;104:1604–1609.
47. Freedland SJ, Humphreys EB, Mangold LA, Eisenberger M, Dorey FJ, Walsh PC, Partin AW. Death in patients with recurrent prostate cancer after radical prostatectomy: Prostate-specific antigen doubling time subgroups and their associated contributions to all-cause mortality. J Clin Oncol 2007;25:1765–1771.
48. Ponud CR, Partin AW, Eisenberger M, Chan DW, Pearson JD, Walsh PC. Natural history of progression after PSA elevation following radical prostatectomy. JAMA 1999;281:1591–1597.
49. Stewart AJ, Scher HI, Chen MH, McLeod DG, Carroll PR, Moul JW, D'Amico AV. Prostate-specific antigen nadir and cancer-specific mortality following hormonal therapy for prostate-specific antigen failure. J Clin Oncol 2005;23:6556–6560.
50. Ward JF, Zincke H, Bergstralh EJ, Slezak JM, Blute ML. Prostate specific antigen doubling time subsequent to radical prostatectomy as a prognosticator of outcome following salvage radiotherapy. J Urol 2004;172:2244–2248.
51. Ings RMJ. Interspecies scaling and comparisons in drug development and toxicokinetics. Xenobiotica 1990;20:1201–1231.
52. Travis CC, White RK. Interspecific scaling of toxicity data. Risk Anal 1988;8:119–125.
53. Rhomberg LR, Lewandowski TA. Methods for identifying a default cross-species scaling factor. http://www.epagov/raf/publications/pdfs/RHOMBERGSPAPERPDF. 2004.

Cancer Science The official journal of the Japanese Cancer Association JCA

Purple corn color inhibition of prostate carcinogenesis by targeting cell growth pathways

Ne Long,[1] Shugo Suzuki,[1] Shinya Sato,[1] Aya Naiki-Ito,[1] Keisuke Sakatani,[2] Tomoyuki Shirai[1,3] and Satoru Takahashi[1,4]

[1]Department of Experimental Pathology and Tumor Biology, Nagoya City University Graduate School of Medical Sciences, Nagoya; [2]Food Color Laboratory, San-Ei Gen F.F.I., Inc., Osaka; [3]Nagoya City Rehabilitation Center, Nagoya, Japan

(Received September 24, 2012/Revised November 5, 2012/Accepted November 20, 2012/Accepted manuscript online November 30, 2012/Article first published online January 20, 2013)

Purple corn color is a widely used food colorant that was reported to have attenuating effects on hypertension, diabetes, and to have anti-cancer effects on colon and breast cancer. Our study is the first on its possible chemoprevention effects against prostate cancer. For this purpose an androgen-dependent prostate cancer cell line, LNCaP, was used to examine effects *in vitro*. Purple corn color inhibited the proliferation of LNCaP cells by decreasing the expression of Cyclin D1 and inhibiting the G1 stage of the cell cycle. Thirty-six male transgenic rats for adenocarcinoma of prostate were fed basic diet or diet with purple corn color for 8 weeks. Purple corn color decreased the incidence of adenocarcinoma in the lateral prostate and slowed down the progression of prostate cancer. A lower Ki67 positive rate, a decrease of the expression of Cyclin D1, and downregulation of the activation of Erk1/2 and p38 MAPK were observed in the group consuming purple corn color in the diet. Since purple corn color is a mixture, determining its active component should help in the understanding and usage of purple corn color for prostate cancer chemoprevention. Therefore, the three major anthocyanins in purple corn color, cyanidin-3-glucoside, pelargonidin-3-glucoside and peonidin-3-glucoside, were tested with LNCaP cells. The results suggested that cyanidin-3-glucoside and pelargonidin-3-glucoside are the active compounds. (*Cancer Sci* 2013; 104: 298–303)

Cancer is a major public health problem in developed and some developing countries. In 2012, prostate cancer (PCa) was estimated to be the No.1 cause of new cancer cases in males and the second highest cause of cancer related deaths in the USA,[1] and PCa is rapidly increasing in Asia. Although considerable effort has been expended on searching for early screening markers and curing PCa, the main treatment remains androgen ablation therapy, which was developed in the early 1940s.[2,3] However, even though more than 80% of PCa respond to this therapy, almost all of these cases relapse in less than a decade and become refractory to treatment.[3] Brachytherapy, radiotherapy, and prostatectomy of PCa prior to metastasis can affect a cure, but these procedures can dramatically alter the quality-of-life of the patient.[4,5] Therefore, prevention of PCa is especially important.

The field of chemoprevention, using natural or laboratory-made substances to prevent cancer, has become increasingly studied in recent years. Researchers have investigated numerous chemicals that may have chemopreventive effects on PCa *in vitro* and *in vivo*. Three large-scale randomized, controlled clinical trials have been conducted: the SELECT trial found that neither selenium nor Vitamin E reduced the risk of PCa in healthy men at average risk;[6] the PCPT trial found that finasteride, a 5α-reductase inhibitor, reduced the risk of PCa of Gleason 6 or less, whereas there was an increased risk of high grade disease with Gleason 7 or more;[7] the REDUCE trial also encountered similar difficulties with dutasteride, another 5 α-reductase inhibitor.[8] Therefore, the search for an appropriate chemopreventor for PCa needs to be continued.

Purple corn has a long history as a food product. Nowadays its color is widely used as a food colorant in Japan. Previous studies have provided evidence that purple corn color (PCC) has anti-cancer effects on colon and breast cancer.[9,10] It also has attenuating effects on some life style diseases, for example, hypertension, hyperglycemia, and diabetes.[11,12] The present study was conducted as an initial investigation on PCC's effects on PCa. As a result we found that PCC inhibited the proliferation of the androgen-dependent cell line LNCaP *in vitro* and inhibited prostate carcinogenesis *in vivo* in the Transgenic Rat for Adenocarcinoma of Prostate (TRAP) model. The TRAP rat model, in which expression of the Simian virus 40 T antigen is under control of the probasin gene promoter, was established in our laboratory. These animals develop high-grade prostatic intraepithelial neoplasia (HG-PIN) and well-differentiated adenocarcinomas with high incidence in all prostate lobes at 15 weeks of age, all lesions being completely androgen-dependent.[13,14] The model provides an ideal tool to gain insights into possible mechanisms of PCa prevention in relatively short-term studies.[15–19]

Purple corn color is a mixture, which contains several anthocynins. To determine its active component, the three major anthocyanins in PCC, cyanidin-3-glucoside (C3G), pelargonidin-3-glucoside (Pg3G) and peonidin-3-glucoside (P3G), were tested using LNCaP cells. By comparing the effects of these anthocyanins to the effect of the mixture, we found that C3G and Pg3G are the active compounds.

To our knowledge, the present study provides the first evidence that PCC inhibits prostate carcinogenesis in a rat model closely mimicking the human disease. The clues obtained as to the molecular basis of action are of critical importance as first steps towards human clinical trials.

Materials and Methods

Chemicals, reagents, plasmids and cell line. Purple corn color was provided by San-Ei Gen F.F.I. (Osaka, Japan). Lot No. 100413, anthocyanin concentration 12.5% was used for the *in vitro* study. Lot No. 110418, anthocyanin concentration 20.9% was used for the *in vivo* study. C3G (Cyanidin-3-O-glucoside chloride) and P3G (Peonidin-3-O-glucoside chloride) were purchased from Tokiwa Phytochemical (Chiba, Japan). Pg3G (Pelargonidin-3-O-glucoside chloride) was purchased from Extrasynthese (Genay Cedex, France). The chemical structures of C3G, P3G and Pg3G are shown in Supplementary

[4]To whom correspondence should be addressed.
E-mail: sattak@med.nagoya-cu.ac.jp

doi: 10.1111/cas.12078

Figure S1. The LNCaP human PCa cell line (androgen-dependent) was from the American Type Culture Collection (Manassas, VA, USA). The pGL3-PSA luciferase expression vector (pGL3/PSA-Luc) was donated by Dr Chawnshang Chang, University of Rochester Medical Center.

Animals. Male heterozygous TRAP rats with a Sprague–Dawley genetic background were used in the present study. They housed three animals per cage on wood-chip bedding in an air-conditioned animal room at 23 ± 2°C and 50 ± 10% humidity. Food and tap water were available *ad libitum*. The Institutional Animal Care and Use Committees of the Nagoya City University (Nagoya, Japan) specifically approved this study.

Experimental protocol. A total of 36 heterozygous male TRAP rats at 6 weeks of age were randomly divided into three groups. Rats in the control group (n = 13) received powdered basal diet (Oriental MF, Oriental Yeast, Tokyo, Japan). The rats in the other two groups received 0.1% (n = 12) or 1% PCC (n = 11) in the diet for 8 weeks. At the end of week 8, the rats were killed under deep anesthesia. Each prostate was removed and halves of the ventral and lateral lobes were immediately frozen in liquid nitrogen and stored at −80°C until processed; the remaining prostates was fixed in 10% neutral buffered formalin, embedded in paraffin, and sectioned. Testosterone and estrogen levels in the serum were analyzed by radioimmunoassay by SRL (Tokyo, Japan). All experiments were performed under protocols approved by the Institutional Animal Care and Use Committee of Nagoya City University Graduate School of Medical Sciences.

Assessment of prostate neoplastic lesion development. Neoplastic lesions in the prostate glands of TRAP rats were evaluated as previously described.[19] Briefly, neoplastic lesions were classified into three types: low-grade prostatic intraepithelial neoplasia (LG-PIN), HG-PIN and adenocarcinoma. The relative numbers of acini with the histological characteristics of each type, that is, LG-PIN, HG-PIN and adenocarcinoma, were quantified with reference to the total acini in each prostatic lobe.

Immunoblot analysis. The immunoblotting analysis was performed as described previously.[19] Briefly, LNCaP cells or frozen ventral prostate tissues were homogenized in radioimmunoprecipitation assay buffer (150 mM NaCl, 50 mM Tris–HCl [pH 8.0], 1% NP-40, 0.5% sodium deoxycholate, 0.1% SDS, 1 mM phenylmethylsulphonyl fluoride, 1 mM sodium orthovanadate, and protease inhibitor cocktail [Complete, Roche, Mannheim, Germany]) and subjected to immunoblot analysis using standard techniques. The antibodies used were Cyclin D1 and androgen receptor (Santa Cruz Biotechnology, Santa Cruz, CA, USA), cleaved caspase 3, cleaved caspase 7, Erk1/2, phospho-Erk1/2, p38 MAPK and phospho-p38 MAPK (Cell Signaling Technology, Boston, MA, USA), prostate-specific antigen (DAKO, Tokyo, Japan) and β-actin (Sigma-Aldrich, St. Louis, MO, USA). The density of the bands was semi-quantified using ImageJ (version 1.42q, National Institute of Health, Bethesda, MD, USA).

Immunohistochemistry. Deparaffinized sections were incubated with antibodies for Ki-67 (Novocastra Laboratories, Newcastle, UK) and SV40 T antigen (Santa Cruz Biotechnologies). Apoptotic cells in the prostate were detected using an *In Situ* Apoptosis Detection kit (TUNEL method) according to the manufacturer's instructions (Takara Bio, Ohtsu, Japan). Labeling indices were determined as the positive percentage for Ki-67 or TUNEL by randomly picking eight fields of view in the whole ventral/lateral prostate and counting over 1000 prostate epithelial cells under a microscope at high magnification.

Cell proliferation assay. Cell proliferation of LNCaP cells was assessed by manual counting under trypan blue staining. Briefly, LNCaP cells were seeded in 96-well plates at 10 000 cells/well in 200 μL of RPMI media; PCC, C3G, Pg3G or P3G were added 24 h after seeding and the cells were incubated for 72 h; and the cells were removed from the plate with trypsin-EDTA and counted.

RNA extraction, cDNA preparation, and quantitative real-time PCR. Total RNAs of LNCaP cells or frozen prostate tissue was isolated using an RNeasy Mini kit (Qiagen, Valencia, CA, USA) and reverse-transcribed with the Thermoscript first-strand synthesis system (Invitrogen Corporation, Carlsbad, CA, USA). Real-time RT-PCR was performed using Syber Premix Ex Taq II (Takara) in a LightCycler (Roche Diagnostics GmbH). The primers used were: human GAPDH, 60°C, 5′-AACGGATTTGGTCGTATTGG-3′ and 5′-CATACTTCTCATGGTTCACA-3′; human Cyclin D1, 60°C, 5′-CCGAGAAGCTGTGCATCTAC-3′ and 5′-CAGGTTCAGGCCTTGCACTG-3′; rat GAPDH, 59°C, 5′-GAATGGGAAGCTGGTCATCA-3′ and 5′-TGGATGCAGGGATGATGTTC-3′; rat probasin, 60°C, 5′-ACTTCCGTCGCATTGAGTGT-3′ and 5′-GTAAACGTCTTGGGATCTCC-3′; rat GK11, 59°C, 5′-GCAGCACCAAACCCCTGGAT-3′ and 5′-TGAGATCTGTCACCTTCTCA-3′.

Cell cycle analysis. LNCaP cells were seeded in 6-well plates at 150 000 cells/well. Purple corn color, C3G or Pg3G were added 24 h after seeding, incubated for 72 h, collected and analyzed with propidium iodide (Guava cell cycle reagent; Guava Technologies, Hayward, CA, USA) according to the Guava Cell Cycle Assay protocol. The cell cycle phase distribution was determined on a Guava PCA Instrument using CytoSoft Software.

Reporter gene assays. LNCaP cells were transfected with the pGL3/PSA-Luc using Nucleofector II. 24 h later, 5 nM DHT and/or PCC were added. After 48 h incubation, the cells were lysed with the buffer supplied in the kit. Luciferase assays were conducted using the dual-luciferase reporter assay system (Promega, Madison, WI, USA), and the phRL-TK vector (Promega) as an internal control, according to the manufacturer's protocol. Data shown are means and SD of four independent data points.

Statistical analysis. All data presented are mean ± SD values. Statistical comparisons were performed with one-way ANOVA followed by Dunnett's test. Correlations were assessed by Spearman correlation coefficient analysis. A P-value of < 0.05 was considered to be significant. All statistical analyses were performed using GraphPad Prism 5 (GraphPad Software, La Jolla, CA, USA).

Results

PCC inhibition of LNCaP proliferation and slowing of the cell cycle. When the androgen-dependent cell line LNCaP was incubated with increasing levels of PCC for 72 h, the proliferation of the cells was inhibited in a dose-dependent manner (Fig. 1A). Cell cycle analysis showed that PCC increased the proportion of cells in G0/G1 slightly but significantly (Fig. 1B). Western blotting showed a 15–30% decrease in the protein level of Cyclin D1 in the PCC treated cells (Fig. 1C), and reverse-transcription PCR also showed that the mRNA level of Cyclin D1 was significantly decreased by PCC (Fig. 1D). Purple corn color did not affect androgen receptor (AR) expression, but PSA expression was dramatically decreased (Fig. 1C). Since the PSA gene is a target of AR, we used a luciferase assay to examine the influence of PCC on the activity of the PSA promoter. Purple corn color inhibited functional AR transcriptional activity in a dose-dependent manner (Fig. S2).

No toxic effects of PCC were observed in the TRAP rat model. Body weights, relative organ weights (ventral prostate, liver and kidney), and food consumption were not affected by administration of PCC in the diet to TRAP rats (Table S1). The average PCC intakes were 25 mg/rat per day and 267 mg

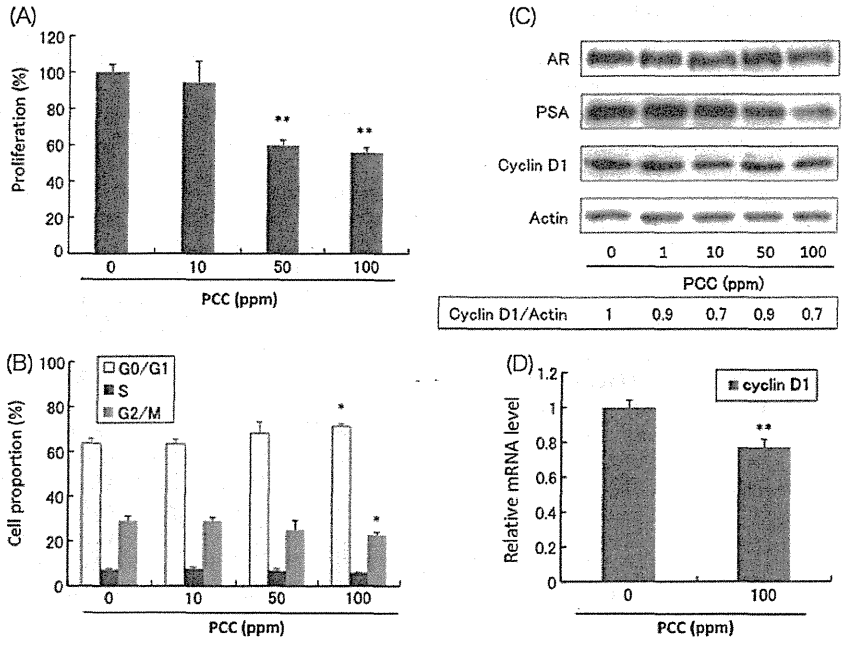

Fig. 1. Effects of purple corn color (PCC) on LNCaP cells. (A) Inhibitory effects on LNCaP cell proliferation (72 h) (n = 3). (B) Effects on the cell cycle of LNCaP cells (n = 3). (C) Protein changes assessed by Western blotting analysis of LNCaP cells after incubation with PCC for 72 h. The density of the bands of Cyclin D1 and actin were semi-quantified by ImageJ. (D) mRNA levels of Cyclin D1 analyzed by reverse-transcription polymerase chain reaction (n = 3). *P < 0.05; **P < 0.01; ***P < 0.001.

/rat per day for the 0.1% and 1% PCC groups (Table S1). Purple corn color did not have any effect on the serum levels of testosterone or estradiol (Table S1).

PCC inhibition of prostate carcinogenesis in the TRAP rat model. With the expression of SV40T antigen under the control of AR, TRAP rats developed prostate cancer with high incidence. In the end of the experiment, all the acini in both ventral and lateral prostate of TRAP rats had developed precancerous or cancerous lesions. Lesions were divided into three stages: LG-PIN, HG-PIN, and adenocarcinoma (Fig. S3). The total percentage of LG-PIN, HG-PIN and adenocarcinoma is 100%. In this study, adenocarcinomas were observed in ventral prostate of all the rats, that is, the incidence of adenocarcinoma was 100% in all three groups. However, the rats consuming PCC had a lower percentage of adenocarcinoma and a higher percentage of LG-PIN (Table 1), which suggests that PCC retarded the progression of PCa and more acini lesions remained in the relatively benign LG-PIN stage. The increased LG-PIN percentage and decreased adenocarcinoma percentage showed a strong correlation to the dose of PCC. In the lateral prostate, we also observed this retardation of PCa progression. Of critical importance in this study is that PCC also significantly decreased the incidence of adenocarcinoma in the lateral prostate (Table 1). These results suggest that PCC inhibited tumorigenesis in the prostates of TRAP rats.

PCC inhibition of the cell growth pathways in the TRAP rat model. Carcinogenesis in the TRAP rat is induced by SV40T antigen expressed under the control of the probasin promoter, which is regulated by the AR. Since PCC downregulated AR activity *in vitro*, we examined whether SV40T expression was downregulated by PCC. Immunohistochemical analysis showed that there was no overt inhibition of SV40T expression by PCC (Fig. 2A,B). We used RT-PCR to examine mRNA levels in the VP of the androgen responsive genes probasin and GK11, an ortholog of human PSA. These results also indicated that AR activity was not inhibited by PCC (Fig. 2C).

Figure 3A shows that the Ki67 index was decreased by PCC in both VP and LP. On the other hand, the TUNEL staining index was not affected by PCC (Fig. 3B), in agreement with our *in vitro* studies in which no apoptosis was observed (data not shown).

Immunoblotting demonstrated factors involved in cell growth pathways, Erk1/2 and p38 MAPK phosphorylation and Cyclin D1, to be downregulated by PCC. In agreement with the results of TUNEL staining, PCC had no affect on the levels of cleaved caspases 3 or 7 (Fig. 3C).

Search for active compounds in PCC. The compounds that give PCC its purple color are anthocyanins. C3G, Pg3G and P3G are the three major components of PCC. When their effects on LNCaP cells were tested, C3G and Pg3G dose-dependently inhibited the proliferation of LNCaP cells, while P3G had no effect (Fig. 4A). The differences of the chemical structures of these three chemicals (Fig. S1) suggest that the hydroxyl radical may play an important role in the inhibitory activity on PCa. Both C3G and Pg3G upregulated AR expression. However, PSA expression, an indicator of AR activity, remained the same (Fig. 4B). This effect on AR activity is in contrast to the effect of PCC *in vitro* but similar to that *in vivo*. Both C3G and Pg3G decreased the expression of Cyclin D1 (Fig. 4C), while increasing the proportion of cells in G0/G1 (Fig. 4D,E), again in line with the PCC effect.

Discussion

Purple corn color is reported to have anti-cancer effect on colon and breast cancer,[9,10] and it also has attenuating effects on some life style diseases, for example, hypertension, hyperglycemia, and diabetes.[11,12] Like breast cancer, PCa is hormone-related. Prostate cancer is also closely associated with a high-fat diet.[20,21] Finally, in the TRAP model, hypertension is positively associated with PCa development.[22] Therefore, we investigated the possibility that PCC could have inhibitory effects on PCa. The results of our experiments, both *in vitro* and *in vivo*, supported this hypothesis. Purple corn color not only showed antiproliferative effects on an androgen-dependent PCa cell line, it also inhibited prostate carcinogenesis *in vivo*. Importantly, dietary PCC did not have any observable toxic effects: there were no significant changes in the final body weights or relative liver or kidney weights in rats fed PCC in their diets. This suggests that PCC could be used as a long-term dietary supplement for chemoprevention of PCa. The success of PCC in the TRAP

doi: 10.1111/cas.12078

Table 1. Quantitative evaluation of neoplastic lesions in prostates of TRAP rats treated with PCC

	No. of animal	Incidence of adenocarcinoma	Proportion of acini in different stages of carcinogenesis (%)		
			LG-PIN	HG-PIN	Adenocarcinoma
Ventral prostate					
Control	13	13 (100%)	4.4 ± 2.8	89.2 ± 3.5	6.4 ± 4.0
0.1% PCC	12	12 (100%)	5.9 ± 3.4**	90.6 ± 3.8	3.5 ± 1.7***
1% PCC	11	11 (100%)	9.1 ± 3.9**	88.2 ± 3.4	2.7 ± 2.0***
Lateral prostate					
Control	13	12 (92%)	24.7 ± 12.4	72.8 ± 11.7	2.5 ± 2.8
0.1% PCC	12	7 (58%)	17.8 ± 5.6	81.2 ± 5.6	1.0 ± 1.0**
1% PCC	11	3 (27%)*	21.1 ± 6.8	78.0 ± 6.2	0.9 ± 1.6**

AC, adenocarcinoma; HG, high grade; LG-PIN, low grade prostatic intraepithelial neoplasia. *P < 0.01 versus control (Dunnett's test). **P < 0.01 and ***P < 0.001 versus control, respectively (Spearman's rank correlation coefficient analysis).

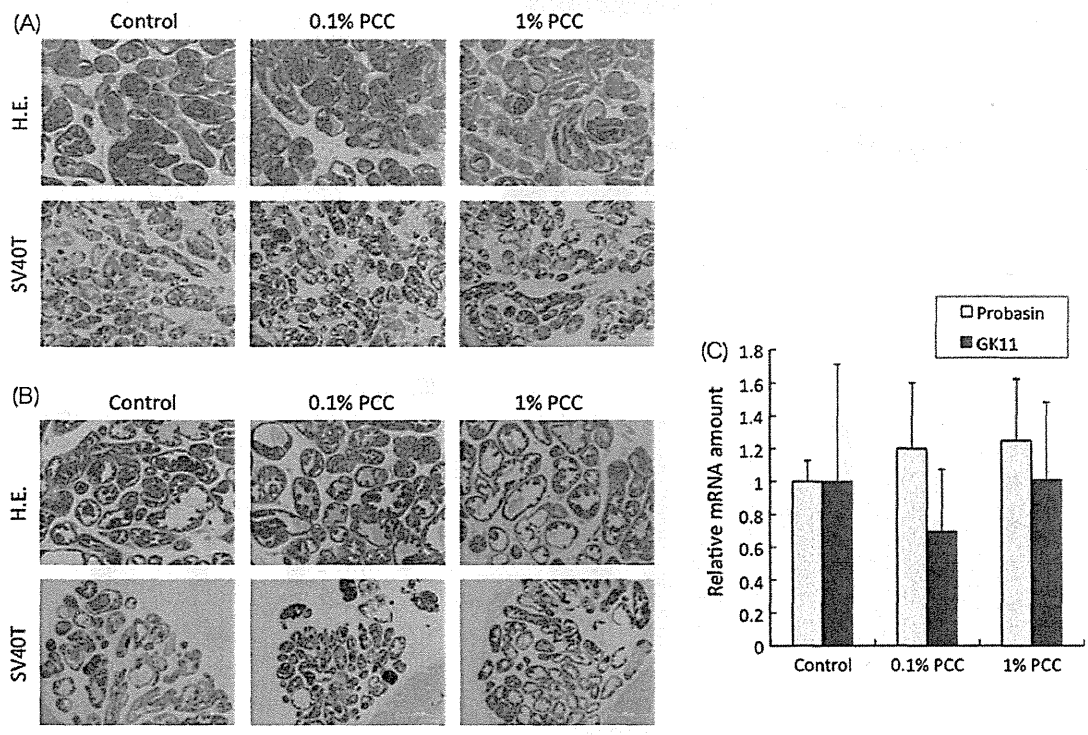

Fig. 2. Purple corn color (PCC)-mediated inhibition of carcinogenesis is not due to down regulation of androgen receptor (AR) activity. (A) H&E staining (4 9 magnification) and SV40T antigen expression (4 9 magnification) in the ventral prostate. (B) H&E staining (4 9 magnification) and SV40T antigen expression (4 9 magnification) in the lateral prostate. (C) mRNA of the ventral prostate was used for reverse-transcription polymerase chain reaction. mRNA levels of probasin and GK11 (the rat ortholog of human PSA), which are AR target genes, were checked. Scale bars, 500 μm.

rat model demonstrates that PCC may inhibit prostate carcinogenesis not only in a simple *in vitro* tissue culture system but also in the complex system of living experimental animals.

To date, an enormous effort has been made to find means to prevent PCa, but an ideal chemopreventor active by itself has yet to be found. The trend has therefore been to put chemicals that target different pathways together to form a "cocktail" that would be more effective. Our laboratory has been focused on looking for PCa chemopreventors. We previously reported that resveratrol could inhibit PCa genesis by targeting the AR pathway,[19] while γ-tocopherol exerts inhibitory effects though activation of caspase-signaling.[23] In the present study, we found that PCC targets cell growth. A reasonable expectation is that combining PCC, resveratrol and γ-tocopherol could have a greater effect than using any of the compounds singly. This is a direction for future studies.

To better understand the chemopreventive effects of PCC on PCa, identifying the active components is essential. Cell proliferation assays here indicated that both C3G and Pg3G dose-dependently inhibited the growth of LNCaP. Similarly to PCC, both C3G and Pg3G decreased the expression of Cyclin D1 and increased the percentage of LNCaP cells in G0/G1. The increased percentage of cells in G0/G1 was about 1.1 times compared to the control. Importantly, the cell proliferation was inhibited by approximately 50%. This suggests that while the effect of C3G and Pg3G on the cell proliferation is rather small, the cumulative effect over time can be substantial. Intriguingly, although the PCC mixture downregulated AR activity, C3G and Pg3G did not show the same effect. Notably, PCC inhibited carcinogenesis in the TRAP model without

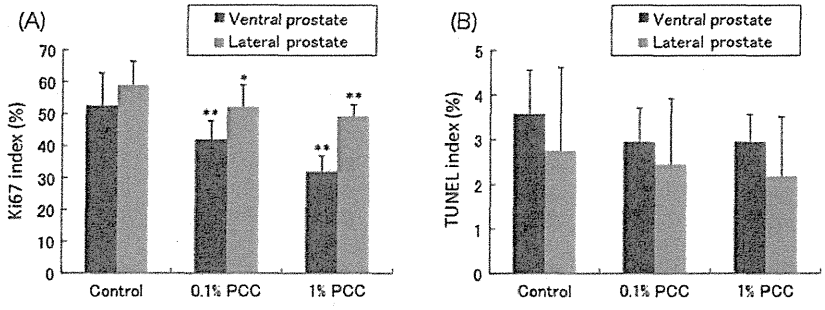

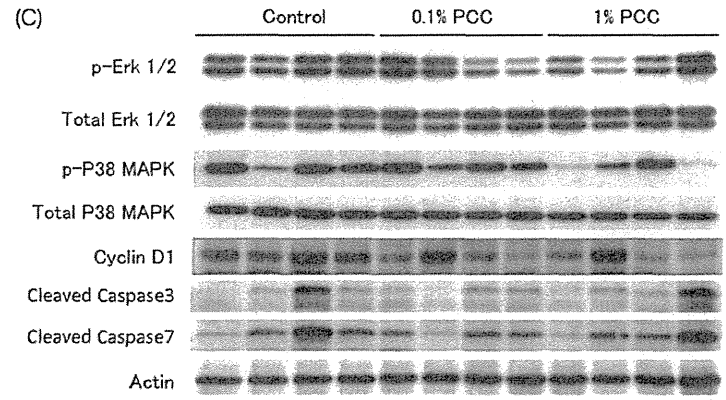

Fig. 3. Effects of purple corn color (PCC) on Ki67 and terminal deoxynucleotidyl transferase-mediated dUTP nick end labeling (TUNEL) indices in the prostate. (A) Purple corn color decreased the Ki67 index significantly in both the ventral and lateral prostate (samples from all the rats were used for analysis). (B) Purple corn color did not affect the TUNEL index in either the ventral or lateral prostate (samples from all the rats were used for analysis). (C) Western blot of proteins related to cell growth and apoptosis using samples from the ventral prostate.

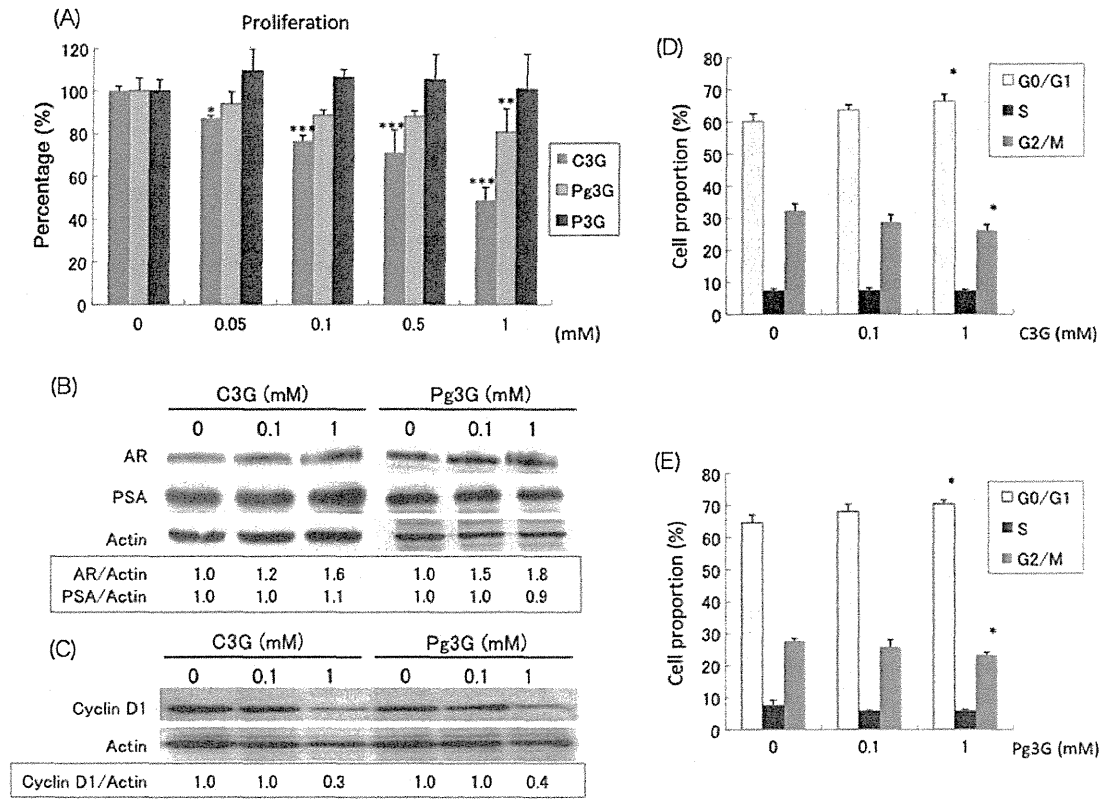

Fig. 4. Anthocyanins in the purple corn color (PCC) mixture, cyanidin-3-glucoside (C3G), pelargonidin-3-glucoside (Pg3G) and peonidin-3-glucoside (P3G), were tested using LNCaP cells. (A) Effects of C3G, Pg3G and P3G on LNCaP cell proliferation. (B,C) Findings of Western blotting. The density of the bands of androgen receptor (AR), PSA and actin were semi-quantified by ImageJ. (D) Effects of C3G on the cell cycle of LNCaP cells. (E) Effects of Pg3G on the cell cycle of LNCaP cells. $*P < 0.05$; $**P < 0.01$; $***P < 0.001$.

downregulating AR activity. Therefore, it is likely that PCC does not inhibit PCa through downregulation of AR. The downregulation observed with the PCC mixture *in vitro* might be a byproduct of other compounds. Taken together, these results suggest that C3G and Pg3G are the probable active compounds contained in PCC.

doi: 10.1111/cas.12078

Carcinogenesis is a complex and long-term progress. Therefore, finding a chemopreventor and using it to inhibit the progression of PCa will be of general benefit. Our study has proved: (i) the safety of relatively long-term PCC consumption; (ii) PCC can inhibit PCa both *in vitro* and *in vivo*, and modulation of cell growth pathways may possibly be involved in suppressive effects of PCC. Other studies have reported that C3G and Pg3G, the active compounds in PCC, have antioxidant and free-radical-scavenging effects, which may protect cells from oxidative damage and reduce the risk of diabetes, cardiovascular diseases and cancer.[24–27] With further study, we can expect to determine whether the mechanism of PCC inhibition of PCa also involves these pathways. Modulation of multiple pathways can increase the chance of PCC effectively preventing PCa in humans. Taking the available information into account, PCC, a widely used food colorant, appears to be a promising chemopreventor for PCa.

Acknowledgments

This work was supported by a Grant-in-Aid for the 3rd Term Comprehensive 10-year Strategy for Cancer Control from the Ministry of Health, Labour and Welfare of Japan and a grant from the Society for Promotion of Pathology of Nagoya, Japan. The authors thank Koji Kato and Junko Takekawa for their technical assistance with immunohistochemistry.

Disclosure Statement

The authors have no conflict of interest.

References

1 Siegel R, Naishadham D, Jemal A. Cancer statistics, 2012. *CA Cancer J Clin* 2012; 62: 10–29.
2 Huggins C, Hodges CV. The effect of castration, of estrogen and of androgen injection on serum phosphatases in metastatic carcinoma of the prostate. *Cancer Res* 1941; 1: 293–7.
3 Rubin MA. Targeted therapy of cancer: new roles for pathologists-prostate cancer. *Mod Pathol* 2008; 21(Suppl. 2): S44–55.
4 Wei JT, Dunn RL, Sandler HM *et al.* Comprehensive comparison of health-related quality of life after contemporary therapies for localized prostate cancer. *J Clin Oncol* 2002; 20: 557–66.
5 Sanda MG, Dunn RL, Michalski J *et al.* Quality of life and satisfaction with outcome among prostate-cancer survivors. *N Engl J Med* 2008; 358: 1250–61.
6 Lippman SM, Klein EA, Goodman PJ *et al.* Effect of selenium and vitamin E on risk of prostate cancer and other cancers: the selenium and vitamin E cancer prevention trial (SELECT). *JAMA* 2009; 301: 39–51.
7 Thompson IM, Tangen CM, Goodman PJ, Lucia MS, Klein EA. Chemoprevention of prostate cancer. *J Urol* 2009; 182(2): 499–507; discussion 508.
8 Andriole GL, Bostwick DG, Brawley OW *et al.* Effect of dutasteride on the risk of prostate cancer. *N Engl J Med* 2010; 362: 1192–202.
9 Hagiwara A, Miyashita K, Nakanishi T *et al.* Pronounced inhibition by a natural anthocyanin, purple corn color, of 2-amino-1-methyl-6-phenylimidazo [4,5-b]pyridine (PhIP)-associated colorectal carcinogenesis in male F344 rats pretreated with 1,2-dimethylhydrazine. *Cancer Lett* 2001; 171: 17–25.
10 Fukamachi K, Imada T, Ohshima Y, Xu J, Tsuda H. Purple corn color suppresses Ras protein level and inhibits 7,12-dimethylbenz[a]anthracene-induced mammary carcinogenesis in the rat. *Cancer Sci* 2008; 99: 1841–6.
11 Shindo M, Kasai T, Abe A, Kondo Y. Effects of dietary administration of plant-derived anthocyanin-rich colors to spontaneously hypertensive rats. *J Nutr Sci Vitaminol (Tokyo)* 2007; 53: 90–3.
12 Tsuda T, Horio F, Uchida K, Aoki H, Osawa T. Dietary cyanidin 3-O-beta-D-glucoside-rich purple corn color prevents obesity and ameliorates hyperglycemia in mice. *J Nutr* 2003; 133: 2125–30.
13 Asamoto M, Hokaiwado N, Cho YM *et al.* Prostate carcinomas developing in transgenic rats with SV40 T antigen expression under probasin promoter control are strictly androgen dependent. *Cancer Res* 2001; 61: 4693–700.
14 Cho YM, Takahashi S, Asamoto M *et al.* Age-dependent histopathological findings in the prostate of probasin/SV40 T antigen transgenic rats: lack of influence of carcinogen or testosterone treatment. *Cancer Sci* 2003; 94: 153–7.
15 Zeng Y, Yokohira M, Saoo K *et al.* Inhibition of prostate carcinogenesis in probasin/SV40 T antigen transgenic rats by raloxifene, an antiestrogen with anti-androgen action, but not nimesulide, a selective cyclooxygenase-2 inhibitor. *Carcinogenesis* 2005; 26: 1109–16.
16 Kandori H, Suzuki S, Asamoto M *et al.* Influence of atrazine administration and reduction of calorie intake on prostate carcinogenesis in probasin/SV40 T antigen transgenic rats. *Cancer Sci* 2005; 96: 221–6.
17 Said MM, Hokaiwado N, Tang M *et al.* Inhibition of prostate carcinogenesis in probasin/SV40 T antigen transgenic rats by leuprorelin, a luteinizing hormone-releasing hormone agonist. *Cancer Sci* 2006; 97: 459–67.
18 Tang M, Ogawa K, Asamoto M *et al.* Protective effects of citrus nobiletin and auraptene in transgenic rats developing adenocarcinoma of the prostate (TRAP) and human prostate carcinoma cells. *Cancer Sci* 2007; 98: 471–7.
19 Seeni A, Takahashi S, Takeshita K *et al.* Suppression of prostate cancer growth by resveratrol in the transgenic rat for adenocarcinoma of prostate (TRAP) model. *Asian Pac J Cancer Prev* 2008; 9: 7–14.
20 De Nunzio C, Aronson W, Freedland SJ, Giovannucci E, Parsons JK. The correlation between metabolic syndrome and prostatic diseases. *Eur Urol* 2012; 61: 560–70.
21 Hoda MR, Mohammed N, Theil G, Fischer K, Fornara P. Obesity and prostate cancer: role of adipocytokines and clinical implications. *Urologe A* 2012; 51: 1253–60.
22 Takeshita K, Takahashi S, Tang M, Seeni A, Asamoto M, Shirai T. Hypertension is positively associated with prostate cancer development in the TRAP transgenic rat model. *Pathol Int* 2011; 61: 202–9.
23 Takahashi S, Takeshita K, Seeni A *et al.* Suppression of prostate cancer in a transgenic rat model via gamma-tocopherol activation of caspase signaling. *Prostate* 2009; 69: 644–51.
24 Sun CD, Zhang B, Zhang JK *et al.* Cyanidin-3-glucoside-rich extract from Chinese bayberry fruit protects pancreatic beta cells and ameliorates hyperglycemia in streptozotocin-induced diabetic mice. *J Med Food* 2012; 15: 288–98.
25 Delazar A, Khodaie L, Afshar J, Nahar L, Sarker SD. Isolation and free-radical-scavenging properties of cyanidin 3-O-glycosides from the fruits of Ribes biebersteinii *Berl. Acta Pharm* 2010; 60: 1–11.
26 Xu M, Bower KA, Wang S *et al.* Cyanidin-3-glucoside inhibits ethanol-induced invasion of breast cancer cells overexpressing ErbB2. *Mol Cancer* 2010; 9: 285.
27 Goulas V, Manganaris GA. The effect of postharvest ripening on strawberry bioactive composition and antioxidant potential. *J Sci Food Agric* 2011; 91: 1907–14.

Supporting Information

Additional Supporting Information may be found in the online version of this article:

Fig. S1. The chemical structures of C3G, Pg3G and P3G.

Fig. S2. PCC down regulated the activity of the PSA promoter.

Fig. S3. The different stages of carcinogenesis in the prostate of TRAP rat.

Table S1. Final body and organ weights, serum hormone levels, and average PCC intake.

Experimental and Toxicologic Pathology 65 (2013) 1035–1041

Contents lists available at ScienceDirect

Experimental and Toxicologic Pathology

journal homepage: www.elsevier.de/etp

Apocynin, an NADPH oxidase inhibitor, suppresses progression of prostate cancer via Rac1 dephosphorylation

Shugo Suzuki[a,b,*], Pornsiri Pitchakarn[a,c], Shinya Sato[a], Tomoyuki Shirai[a], Satoru Takahashi[a]

[a] Department of Experimental Pathology and Tumor Biology, Graduate School of Medicine, Nagoya City University, Nagoya, Japan
[b] Pathology Division, Nagoya City East Medical Center, Nagoya, Japan
[c] Department of Biochemistry, Faculty of Medicine, Chiang Mai University, Chiang Mai, Thailand

ARTICLE INFO

Article history:
Received 8 January 2013
Accepted 31 March 2013

Keywords:
NADPH oxidase
Prostate cancer
Apocynin
Cancer progression
Rac1

ABSTRACT

Recently, considerable evidence has been generated that oxidative stress contributes to the etiology and pathogenesis of prostate cancer. The present study focused on the effects of apocynin, an inhibitor of the NADPH oxidase which generates intracellular superoxide, on a rat androgen-independent prostate cancer cell line (PLS10) in vitro and in vivo. Apocynin significantly inhibited cell proliferation of PLS10 cells via G1 arrest of the cell cycle in vitro. Surprisingly, it did not affect reactive oxygen species (ROS) but inhibited phosphorylation of Rac1, one component of the NADPH oxidase complex. A Rac1 inhibitor, NSC23766, also inhibited cell proliferation, and both apocynin and NSC23766 reduced phosphorylation of Rac1 and NF-κB, as well as cyclin D1. Furthermore, in a xenograft model of prostate cancer with PLS10, apocynin suppressed tumor growth and metastasis in a dose dependent manner in vivo, with reduction of cell proliferation and vessel number in the tumors. Expression and secretion of vascular endothelial growth factor (VEGF) were reduced by apocynin treatment in vivo and in vitro, respectively. In conclusion, despite no apparent direct relationship with oxidative stress, apocynin inhibited growth of androgen-independent prostate cancer in vitro and in vivo. Apocynin thus warrants further attention as a potential anti-tumor drug.

1. Introduction

Prostate cancer is the second most frequently diagnosed cancer in males in the world, with especially higher incidences in Oceania, Europe and North America. In Japan, incident and mortality rates of prostate cancer are relatively low but increasing (Jemal et al., 2011; Damber and Aus, 2008). Androgen ablation therapy is a widely used treatment during the initial stage of the disease and may produce an initially favorable outcome, but most patients eventually develop androgen-independent prostate cancers with metastatic foci, which cause patient death. Currently, there is no therapy that is able to cure progressive hormone-refractory metastatic prostate cancer (Damber and Aus, 2008). New therapeutic agents are thus needed urgently.

Reactive oxygen species (ROS) can be important factors for carcinogenesis and tumor progression, not only inducing DNA damage but also producing cellular alterations such as up-regulation of mitogen activated protein kinase (MAPK) and protein kinase C (PKC) (Lee et al., 2006; Wu, 2006). Recently, considerable evidence has been published suggesting oxidative stress contributes to the etiology and pathogenesis of the prostate cancer (Kumar et al., 2008; Khandrika et al., 2009). Therefore, we have focused on inhibition of ROS production as an anti-tumor approach for prostate cancer.

ROS is produced by mitochondria, peroxisomes, cytochrome P-450, and other cellular elements as a by-product, generated by nicotinamide adenine dinucleotide phosphate (NADPH) oxidase, which is also implicated in a variety of signaling events, including cell growth, cell survival and cell death (Bedard and Krause, 2007). NADPH oxidase consists of phox units ($gp91^{phox}$, $p22^{phox}$, $p40^{phox}$, $p47^{phox}$, $p67^{phox}$) and Rac, the small molecular weight G protein (Bedard and Krause, 2007). Apocynin, a methoxy-substituted catechol that inhibits NADPH oxidase by blocking the association of $p47^{phox}$ and $p67^{phox}$ with $gp91^{phox}$ (Stolk et al., 1994), is now used as a standard NOX inhibitor for research purposes (Bedard and Krause, 2007). Additionally, apocynin can be converted by peroxidase-mediated oxidation to a dimer, which has been shown to be more efficient inhibitor than apocynin itself (Stefanska and Pawliczak, 2008). We previously presented evidence that apocynin reduced oxidative stress induced by arsenite treatment of rat urothelium in vivo (Suzuki et al., 2009).

In the present study we focused on NADPH oxidase and tested whether its inhibitor, apocynin, might be able suppression of androgen-independent prostate cancer progression in vitro

* Corresponding author at: Nagoya City University Graduate School of Medical Sciences, 1 Kawasumi, Mizuho-cho, Mizuho-ku, Nagoya 467-8601, Japan.
Tel.: +81 52 853 8156; fax: +81 52 842 0817.
E-mail address: shugo@med.nagoya-cu.ac.jp (S. Suzuki).

0940-2993/$ – see front matter © 2013 Elsevier GmbH. All rights reserved.
http://dx.doi.org/10.1016/j.etp.2013.03.002

and vivo. The androgen-independent, androgen receptor-negative rat prostate cancer cell line (PLS10), which was established in our laboratory from a 3,2′-dimethyl-4-aminobiphenyl plus testosterone-induced carcinoma in the dorsolateral prostate of a male F344 rat (Nakanishi et al., 1996), was employed for this purpose.

2. Materials and methods

2.1. Cell culture

The PLS10 cell line was cultured in Roswell Park Memorial Institute-1640 Medium (RPMI 1640, Gibco, Carlsbad, CA) with 10% fetal bovine serum (FBS), 50 U/ml penicillin and 50 μg/ml streptomycin, in a humidified incubator with an atmosphere comprising 95% air and 5% CO_2 at 37 °C.

2.2. Animals

All animal experiments were performed under protocols approved by the Institutional Animal Care and Use Committee of Nagoya City University Graduate School of Medical Sciences. Seven-week-old male athymic nude mice (KSN strain) were purchased from Nihon SLC (Hamamatsu, Japan) and housed in plastic cages with hardwood chip bedding in an air-conditioned room at 23 ± 2 °C and 55 ± 5% humidity with a 12 h light/dark cycle. Oriental MF powder diet (Oriental Yeast Co., Tokyo, Japan) and distilled water were available ad libitum.

2.3. Proliferation assay

PLS10 cells were plated at 2.0×10^2 cells per well in 96-well plates. Twenty-four hours after plating, increasing concentrations of apocynin or NSC23766 (Rac1 inhibitor, COSMO BIO Co., Ltd., Tokyo, Japan) were added. The cells were then incubated for 48 h at 37 °C. Cells cultures were observed microscopically and overall cell number/viability was assessed by WST-1 colorimetric assay (Roche Diagnostics, Mannheim, Germany).

2.4. Cell cycle analysis

After starved conditions with 1% bovine serum albumin instead of 10% FBS, the cells were treated with 250 or 500 μM of apocynin for 48 h, then suspensions were prepared and stained with propidium iodide (Guava® cell cycle reagent, Guava Technologies, Hayward, CA) according to the Guava® Cell Cycle Assay protocol. Cell cycle phase distributions were determined on a Guava® PCA Instrument using CytoSoft Software.

2.5. Invasion assay

For invasion assays, cells were seeded in BD Biocoat™ Matrigel™ invasion chambers (BD Biosciences, San Jose, CA), and treated with apocynin (0, 100 and 200 μM) for 24 h 5% FBS was used as a chemoattractant. Invading cells were fixed with 100% ethanol for 5 min, then stained with 0.5% crystal violet in 20% methanol for 30 min. The number of infiltrating cells was counted under a microscope.

2.6. Detection of ROS production

ROS production was detected by a slightly modification of the method described in a previous report (Rosenkranz et al., 1992). Briefly, 24 h after apocynin treatment, culture supernatant was removed from all wells and the cells were washed twice with warm PBS, then 100 μl of 2′,7′-dichlorofluorescin-diacetate (100 μg/ml, DCFH-DA, Sigma) was added with further incubation at 37 °C for 60 min, in the dark. The cells were washed 3 times with warm PBS, and then were lysed in 100 μl of 2.5% TrironX100. After incubation for 5 min, fluorescence intensity was assessed at 485/535 nm with a spectrofluorometer. Images were also recorded with a fluorescence microscope (BZ-9000; Keyence Corp., Osaka, Japan).

2.7. Detection of vascular endothelial growth factor (VEGF) secretion into the medium

PLS10 cells were plated at 6.0×10^4 cells per well in 24-well plate. Twenty-four hours after plating, they were treated with apocynin or NSC23766 for 24 h. The culture medium of each well was transfered to wells of a Rat VEGF Quantikine ELISA Kit (R&D Systems, Inc., Minneapolis, MN), and VEGF secretion into the medium was determined according to the manufacturer's instructions.

2.8. Immunoblot analyses

After treatment of apocynin or NSC23766, cells were washed with ice-cold phosphate buffer saline (PBS) and scraped with a cell scraper into RIPA buffer (Pierce Biotechnology, Rockford, IL) containing a protease inhibitor (Pierce Biotechnology) on ice. The insoluble matter was removed by centrifugation at 12,000 rpm for 20 min at 4 °C and supernatants were collected. Protein concentrations were determined with a Coomassie Plus™-The Better Bradford Assay Kit (Pierce Biotechnology). Samples were mixed with 2× sample buffer (Bio-Rad Laboratories, Hercules, CA) and heated for 5 min at 95 °C and then subjected to 10% SDS-PAGE. The separated proteins were transferred onto nitrocellulose membranes followed by blocking with SuperBlock Blocking Buffer (Thermo Fisher Scientific K.K., Yokohama, Japan) for 1 h at room temperature. Membranes were probed with antibodies for cyclin D1 (Santa Cruz Biotechnology, Inc., Santa Cruz, CA), cleaved caspase-3, Nuclear Factor Kappa B (NF-κB) p65 and phospho-NF-κB p65 (Ser536) (Cell Signaling, Technology Inc., Danvers, MA), Rac1 (Millipore Corporation, Billerica, MA) and phospho-Rac1 (Upstate, Temecula, CA) in 1× TBS with 0.1% Tween-20 at 4 °C overnight, followed by exposure to peroxidase-conjugated appropriate secondary antibodies and visualization with an enhanced chemiluminescence detection system (GE Healthcare Bio-sciences, Buckinghamshire, NA, UK). To confirm equal protein loading, each membrane was stripped and reprobed with anti-β-actin (Sigma–Aldrich, Co., St. Louis, MO). Band densities of cyclin D1, phospho-NF-κB p65 and phospho-Rac1 were then determined with ImageJ 1.410 (National Institute of Mental Health, MD).

2.9. PLS10 xenograft model

After one week of acclimation, mice were divided into 3 groups of 10 mice each. Two hundred thousand of PLS10 cells were mixed with 50% Matrigel (BD Biosciences) and injected (100 μL) subcutaneously into the back area of each mouse. The animals were given drinking water containing 0, 100 and 500 mg/L apocynin for 30 days and body weights and water consumption were estimated every week. The tumor volumes in each mouse were estimated every other day using the following formula: 0.52 (long axis × short axis × short axis). Mice were sacrificed at experimental day 30, when primary tumors and liver, lung, kidneys and lymph nodes were removed and fixed in 10% buffered formalin. Primary tumors were measured and tumor volume was calculated using the following formula: 0.52 (axis1 × axis2 × axis3). At least 1 section of each tissue and the largest section from each lobe of the lung were processed for hematoxylin and eosin staining, immunostaining and

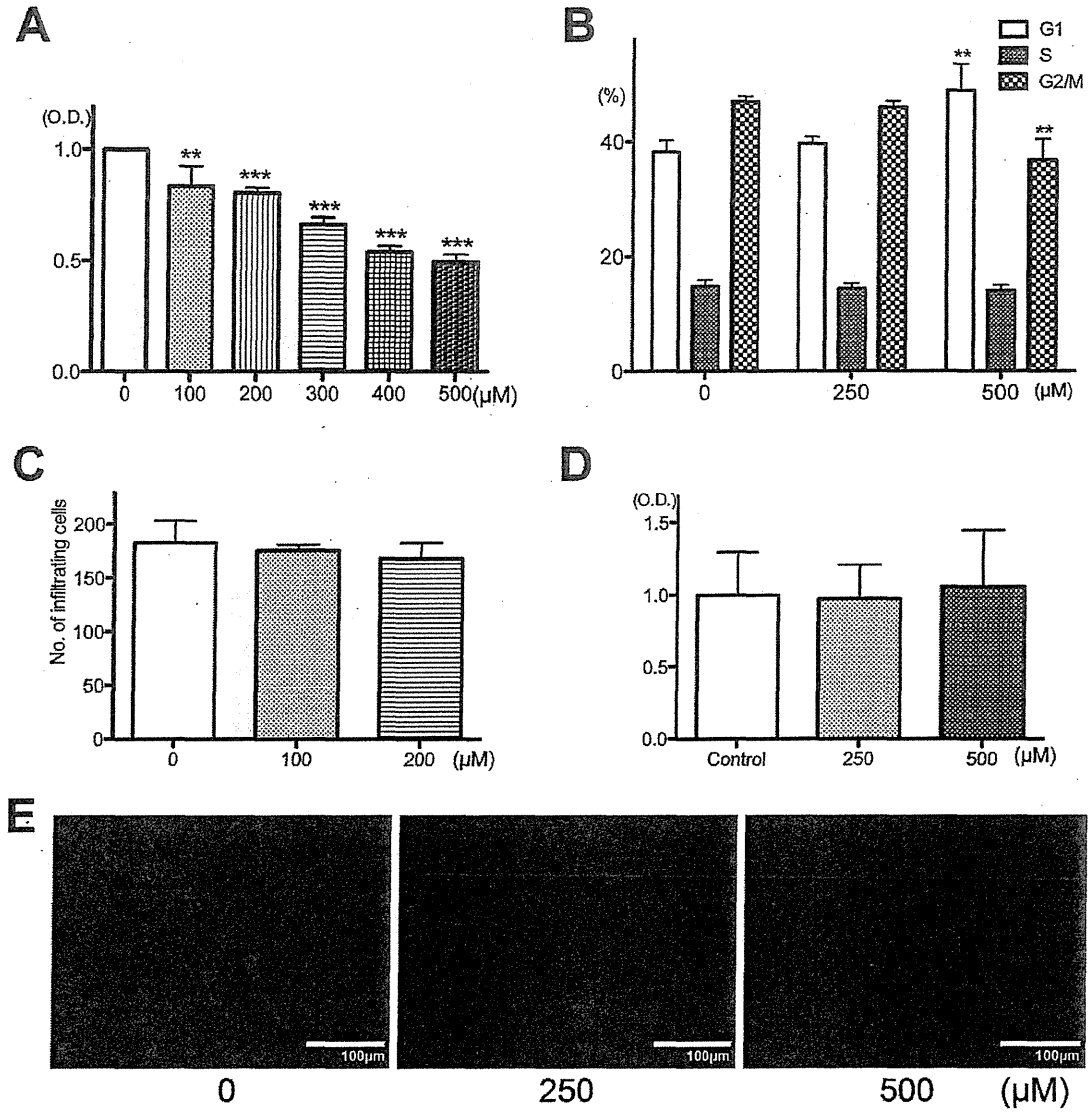

Fig. 1. Apocynin inhibition of cell growth and blockage of cell cycling of PLS10 cells. Cells were incubated with apocynin for 48 h and then cytotoxicity was assessed by WST-1 assay (A). Cell cycle distribution of PLS10 cells after treatment with apocynin for 48 h (B). Cells were treated with 0, 100 and 200 μM apocynin for invasion assays (24 h) using transwell cell culture chambers, with 5% FBS as a chemoattractant (C). ROS production data (D) and photos (E) detected by DCFH-DA after apocynin treatment for 24 h. Data are mean ± SD values from 3 independent experiments. **, ***$P < 0.01$ and 0.001 compared to controls, respectively.

terminal deoxy nucleotidyl transferase-mediated dUTP nick end labeling (TUNEL) assay.

2.10. Immunohistochemistry

Paraffin-embedded specimens were sectioned (3 mm) and stained with Ki67 antibody (SP6; Acris Antibodies GmbH, Herford, Germany), CD31 (Abcam plc, Cambridge, UK), 8-hydroxy-2′-deoxyguanosine (8-OHdG; Nikken SEIL Co., Ltd., Shizuoka, Japan) or Vascular Endothelial Growth Factor (VEGF; Immuno-Biological Laboratories Co., Ltd., Fujioka, Gunma) and then with anti-mouse or -rabbit secondary antibody and avidin–biotin complex (Vectastatin Elite ABC kit; Vector Laboratory, Burlingame, CA), and binding sites were visualized with diamino-benzidine. The sections were then counterstained lightly with hematoxylin for microscopic examination. Staining intensity for VEGF without hematoxylin staining was quantitatively assessed with an Image Processor for Analytical Pathology (IPAP-WIN, Sumika Technos Co., Osaka, Japan) to give optical densities.

2.11. TUNEL assay

Paraffin-embedded specimens were sectioned (3 mm), and apoptotic cells in the tumors were detected by TUNEL assay performed using an In Situ Apoptosis Detection Kit from Takara (Otsu, Japan).

2.12. Statistical analysis

All in vitro experiments were performed at least in triplicate to confirm reproducibility. Statistical analyses were performed with mean ± S.D. values using one-way ANOVA, the Bonferroni correction or Dunnett's test. Statistical significance was concluded at *$P < 0.05$, **$P < 0.01$ or ***$P < 0.001$.

3. Results

WST-1 assay (Fig. 1A) showed that apocynin treatment reduced cell growth of PLS10 cells concentration-dependently after 48 h. At concentrations higher than 100 μM, apocynin treatment significantly inhibited growth, with an inhibitory concentration (IC) 50 of around 500 μM. To explore the underlying mechanism of apocynin-induced growth suppression, cell cycle analysis was performed by Guava® cell cycle assay. Apocynin-treated cells appeared to accumulate in G1 phase, especially at 500 μM (49%, $p < 0.01$), compared to controls (38%), with concomitant decrease in the percentage of cells in the G2/M phase (Fig. 1B). Meanwhile, no significant difference in infiltrating cell number was apparent with/without apocynin treatment in invasion assay (Fig. 1C). Data and photos of ROS detection are presented in Fig. 1D and 1E, respectively. Surprisingly, no significant difference was detected with/without apocynin treatment. Therefore, we investigated another function of the NADPH oxidase complex, and focused on the included Rac1 protein.

Data for expression of Rac-1 and phospho-Rac1 are presented in Fig. 2A. Apocynin treatment only reduced phosphorylation of Rac1 concentration-dependently, but not expression of Rac1. Therefore, we utilized NSC23766, a Rac1 inhibitor, for growth inhibition of PLS10 cells. WST-1 assays indicated that NSC23766 treatment reduced cell growth concentration-dependently after 48 h. At concentrations higher than 10 μM, NSC23766 treatment significantly inhibited growth, with an IC 50 around 200 μM. In the Western blot analysis, both apocynin (500 μM) and NSC23766 (200 μM) treatments reduced phosphorylation of Rac1 and NF-κB p65, and expression of cyclin D1 (Fig. 2C).

During the in vivo experiment, there were no differences in body weight and water consumption among groups (body weight: control, 100 and 500 mg/L apocynin: 27.6 ± 1.8, 27.6 ± 1.6 and 28.4 ± 1.1 g, respectively; water consumption: control, 100 and 500 mg/L apocynin: 4.1 ± 0.2, 4.2 ± 0.2 and 4.1 ± 0.2 ml/mouse/day, respectively). One mouse treated with 500 mg/L apocynin was excluded from the experiment because of spontaneous development of a malignant lymphoma. No toxicity was histologically detected in livers and kidneys of apocynin-treated groups (data not shown), but growth of implanted tumor tended to be reduced (Fig. 3A). Size data and photos of implanted tumors are presented in Fig. 2B and 2C, respectively. Because of individual differences in tumor size, there was no significantly difference between control and apocynin treatment groups overall, but significant reduction was noted with dose-dependence (Spearman's rank correlation coefficient: rho = −0.40, $P < 0.05$). The significant difference between control and 500 mg/L apocynin treatment group was only detected by student T test ($P = 0.0399$). Ki67 labeling indices (Fig. 3D) were significantly reduced by apocynin treatment (100 and 500 mg/L apocynin: 87.7, 86.8%, respectively) in a dose-dependent manner compared to control (90.9%), but TUNEL (Fig. 3E) apoptotic indices were not (control, 100 and 500 mg/L apocynin: 0.88, 0.87 and 0.88%, respectively). To determine antioxidant effects, we investigated the 8-OHdG labeling index (Fig. 3F) but administration of apocynin had no effect (control, 100 and 500 mg/L apocynin: 4.7, 5.0 and 3.8%, respectively). Data for metastatic tumors detected in lungs and/or lymph nodes are presented in Table 1. Apocynin treatment tended to decrease metastatic tumors, but not significantly.

Because reduction of proliferation by apocynin treatment in vivo was relatively slight, we focused on angiogenesis in tumors. Photos and data for numbers of vessels detected with CD31 antibodies are presented in Fig. 4A and B, respectively. The number of vessels per unit tumor area was significantly reduced by apocynin treatment (100 and 500 mg/L apocynin: 185 and 158 mm^{-2}, respectively) compared to control (220 mm^{-2}) with dose-dependence

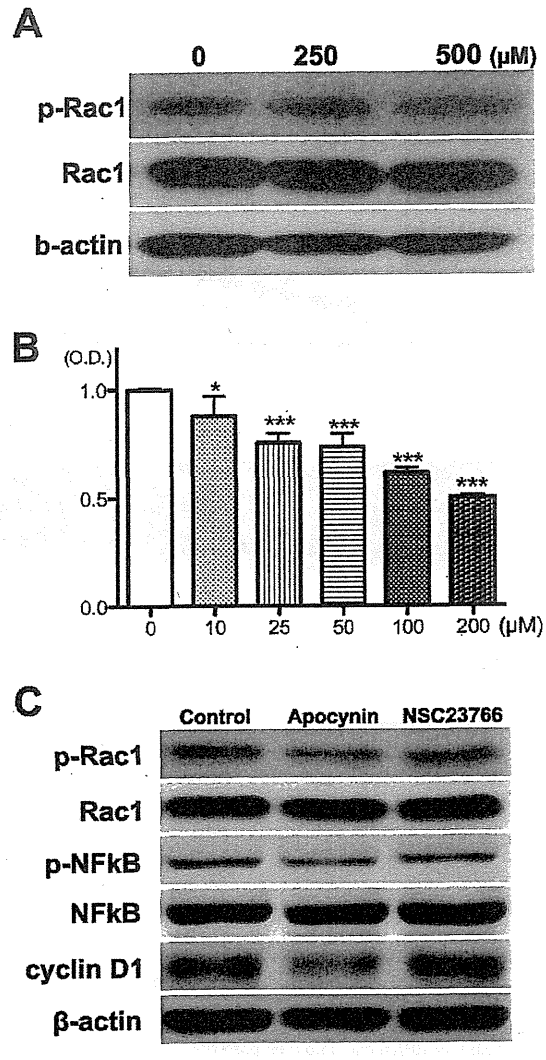

Fig. 2. Apocynin inhibition of phospho-Rac1 in PLS 10 cells. Immunoblot analysis of the protein levels of phosho-Rac1 (p-Rac1), Rac1 and ß-actin (A) with apocynin treatment. The cells were incubated with NSC23766 for 48 h and then cytotoxicity was assessed by WST-1 assay (B). Immunoblot analysis of the protein levels of phosho-Rac1 (p-Rac1), Rac1, phospho-NF-κB (pNF-κB), NF-κB, cyclin D1 and ß-actin (C) with apocynin or NSC23766 treatment. *, ***$P < 0.05$ and 0.001, respectively, compared to 0 μM.

(Spearman's rank correlation coefficient: rho = −0.78, $P < 0.001$). Interestingly, a correlation between tumor size and vessels per tumor was also significant by Spearman's rank correlation coefficient: (rho = 0.52, $P < 0.01$) among all groups. VEGF expression tumor detected by immunostaining was also reduced by apocynin treatment (control, 100 and 500 mg/L apocynin: 1.00, 0.60 and 0.47 optical density, respectively) in a dose-dependent manner (Spearman's rank correlation coefficient: rho = −0.45, $P < 0.05$). In vitro, VEGF secretion from PLS10 cells was significantly reduced by both apocynin and NSC23766 treatments (Fig. 4D).

4. Discussion

In the present study, we demonstrated suppressive effects of apocynin treatment on androgen-independent prostate cancer growth in vitro. Surprisingly, we detected no obvious influence on ROS production but down-regulation of phosphorylated-Rac1 was noted with apocynin treatment, and inhibitory effects were

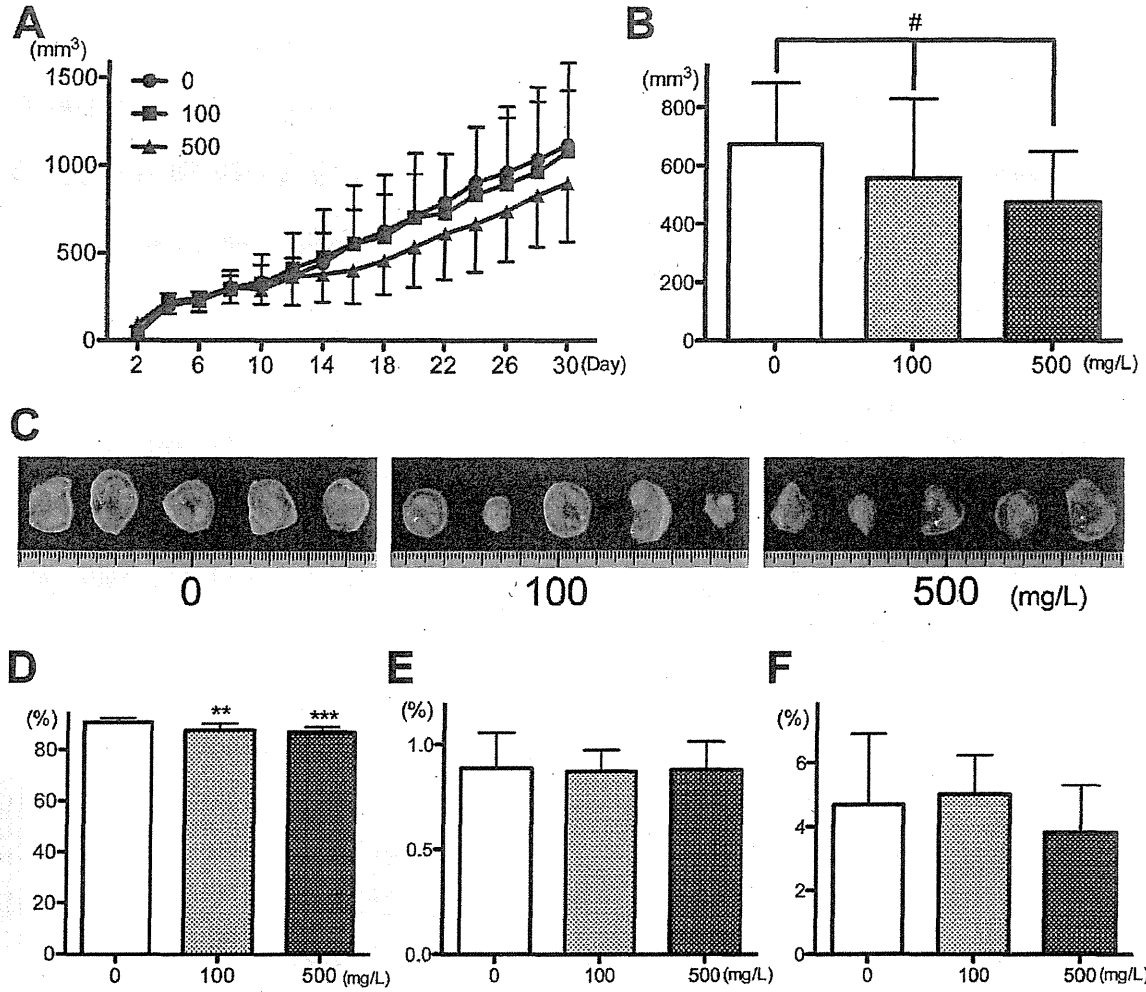

Fig. 3. Apocynin suppression of tumor growth in a PLS10 xenograft model. Nude mice given apocynin (0, 100 and 500 mg/L) in their water were injected subcutaneously with PLS10 cells (2×10^5/animal) into their posterior areas, then sacrificed at day 30. Tumor growth curves (A), data of final tumor size (B), macro photos of tumor (C), Ki67 labeling index (D), percent of TUNEL positive cells (E) and 8-OHdG labeling index are shown. #Spearman's rank correlation coefficient: rho = −0.40, $P < 0.05$, **, ***$P < 0.01$ and 0.001 compared to 0 mg/L, respectively.

confirmed using a Rac1 inhibitor. Rac is a part of the NADPH oxidase complex (Bedard and Krause, 2007), and activated Rac induces NADPH oxidase assembly and activity (Bokoch and Diebold, 2002; Hordijk, 2006). Apocynin is known to block NADPH oxidase assembly (Stolk et al., 1994), and this may be because of reduction of Rac1 activity. More detailed studies are needed to elucidate the mechanism of blocking Rac1 phosphorylation by apocynin.

Concerning human androgen-independent prostate cancer, Kobayashi et al. (2010) demonstrated that activation of Rac1 is related to cell proliferation and androgen-independence. Therefore, the Rac1-regulated pathway appears to be one of the most important for both human and rat androgen-independent prostate cancers, and also an anti-tumor target with apocynin. A number of reports have indicated that prostate cancer cells generate substantial amounts of ROS which are related to cell growth and malignant potential (Kumar et al., 2008; Khandrika et al., 2009). In particular, Kumar et al. (2008) described that another NADPH oxidase inhibitor, diphenyleneiodonium, had the ability to block both ROS production and aggressive potential in some prostate cancer cell lines in vitro.

In vivo, we demonstrated inhibition of implanted tumor growth by apocynin treatment, with reduction of metastatic tumors in lungs and lymph nodes. The dose of apocynin administrated to mice did not cause toxicity, as there were no effects on body weight or water consumption. Interestingly, the inhibitory mechanisms of tumor growth by apocynin appeared related not only with direct effects on cell proliferation but also angiogenesis, as evidenced by decrease of vessels and expression and secretion of

Table 1
Incidence and multiplicity of metastatic tumors in lungs and lymph nodes of xgenograft model.

Treatment	Animal No.	Lung metastasis		Lymph node metastasis	
		Incidence	Multiplicity	Incidence	Multiplicity
Control	10	7	1.40 ± 1.78	2	0.20 ± 0.42
Apocynin 100 mg/L	10	3	0.60 ± 1.07	2	0.20 ± 0.42
Apocynin 500 mg/L	9	3	0.44 ± 0.73	0	0.00 ± 0.00

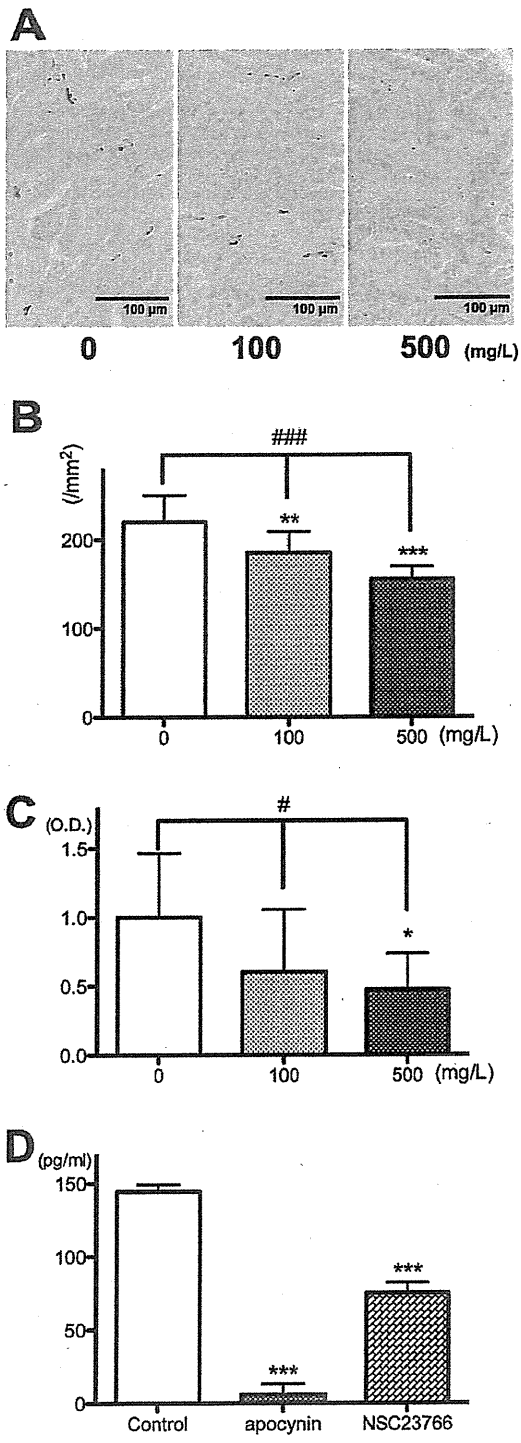

Fig. 4. Relationship between apocynin and angiogenesis. Vessels in the implanted tumors were detected with CD31 antibodies (A), and vessel number per unit area in the tumor are presented (B). VEGF expression in a tumor detected by immunostaining (C). VEGF secretion from PLS10 cells detected by ELISA in vitro (D). ### and #Spearman's rank correlation coefficient: rho = −0.78, $P < 0.001$ and rho = −0.45, $P < 0.05$. *, **, ***$P < 0.01$ and 0.001 compared to 0 mg/L or Control, respectively.

VEGF in tumors. Earlier reports indicated that ROS produced by NADPH oxidase stimulate diverse redox signaling pathways leading to angiogenic responses in endothelial cells and neovascularization in vivo (Ushio-Fukai et al., 2002; Ushio-Fukai, 2006). Therefore, apocynin may have a potential to inhibit tumor growth by blocking angiogenesis directly and indirectly in vivo.

Concerning mechanisms of anti-tumor effects by apocynin in prostate cancer, we detected reduction of NF-κB activation in PLS10 cells. NF-κB is known to be activated in tumor cells and induce cell proliferation, anti-apoptosis, angiogenesis, invasion and/or metastasis in various tumors including human prostate cancer (Prasad et al., 2010; Suh and Rabson, 2004). We found that apocynin inhibited VEGF secretion and cell proliferation via down-regulation of cyclin D1, which might be regulated by NF-κB activation in rat prostate cancer cell lines. Both apocynin and Rac1 inhibitor reduced phosphorylation of NF-κB in line with reports that Rac1 stimulates NF-κB activation in lung and prostate cancers (Sanlioglu et al., 2001; Fan et al., 2009). These data further suggest that the Rac1 pathway is important for prostate cancer development.

In conclusion, apocynin, an NADPH oxidase inhibitor, suppressed tumor growth of androgen-independent prostate cancer in vitro and in vivo. One possible mechanism of action is via Rac1 inactivation. In vivo, apocynin had the potential to inhibit tumor growth directly and indirectly via angiogenesis. Therefore, apocynin warrants further attention as a promising anti-tumor drug for androgen-independent prostate cancer.

5. Conflict of interest

The authors declare no conflict of interest.

Acknowledgements

This work was supported in part by grants from Ono Pharmaceutical Co., Ltd. and the Society for Promotion of Pathology in Nagoya, and the Research Foundation for Oriental Medicine.

References

Bedard K, Krause KH. The NOX family of ROS-generating NADPH oxidases: physiology and pathophysiology. Physiological Reviews 2007;87:245–313.
Bokoch GM, Diebold BA. Current molecular models for NADPH oxidase regulation by Rac GTPase. Blood 2002;100:2692–6.
Damber JE, Aus G. Prostate cancer. Lancet 2008;371:1710–21.
Fan S, Meng Q, Laterra JJ, Rosen EM. Role of Src signal transduction pathways in scatter factor-mediated cellular protection. Journal of Biological Chemistry 2009;284:7561–77.
Hordijk PL. Regulation of NADPH oxidases: the role of Rac proteins. Circulation Research 2006;98:453–62.
Jemal A, Bray F, Center MM, Ferlay J, Ward E, Forman D. Global cancer statistics. CA Cancer Journal for Clinicians 2011;61:69–90.
Khandrika L, Kumar B, Koul S, Maroni P, Koul HK. Oxidative stress in prostate cancer. Cancer Letters 2009;282:125–36.
Kobayashi T, Inoue T, Shimizu Y, Terada N, Maeno A, Kajita Y, Yamasaki T, Kamba T, Toda Y, Mikami Y, Yamada T, Kamoto T, Ogawa O, Nakamura E. Activation of Rac1 is closely related to androgen-independent cell proliferation of prostate cancer cells both in vitro and in vivo. Molecular Endocrinology 2010;24:722–34.
Kumar B, Koul S, Khandrika L, Meacham RB, Koul HK. Oxidative stress is inherent in prostate cancer cells and is required for aggressive phenotype. Cancer Research 2008;68:1777–85.
Lee YJ, Lee JH, Han HJ. Extracellular adenosine triphosphate protects oxidative stress-induced increase of p21(WAF1/Cip1) and p27(Kip1) expression in primary cultured renal proximal tubule cells: role of PI3K and Akt signaling. Journal of Cellular Physiology 2006;209:802–10.
Nakanishi H, Takeuchi S, Kato K, Shimizu S, Kobayashi K, Tatematsu M, Shirai T. Establishment and characterization of three androgen-independent, metastatic carcinoma cell lines from 3,2′-dimethyl-4-aminobiphenyl-induced prostatic tumors in F344 rats. Japanese Journal of Cancer Research 1996;87:1218–26.
Prasad S, Ravindran J, Aggarwal BB. NF-kappaB and cancer: how intimate is this relationship. Molecular and Cellular Biochemistry 2010;336:25–37.
Rosenkranz AR, Schmaldienst S, Stuhlmeier KM, Chen W, Knapp W, Zlabinger GJ. A microplate assay for the detection of oxidative products using 2′,7′-dichlorofluorescin-diacetate. Journal of Immunological Methods 1992;156:39–45.